

Towards a Microscopic Model of Magnetoelectric Interactions in $\text{Ni}_3\text{V}_2\text{O}_8$

A. B. Harris,¹ T. Yildirim,² A. Aharony,^{3,4} and O. Entin-Wohlman,^{3,4}

(1) *Department of Physics and Astronomy, University of Pennsylvania, Philadelphia, PA 19104*

(2) *NIST Center for Neutron Research, National Institute of Standards and Technology, Gaithersburg, Maryland 20899*

(3) *School of Physics and Astronomy, Raymond and Beverly Sackler
Faculty of Exact Sciences, Tel Aviv University, Tel Aviv 69978, Israel*

(4) *Department of Physics, Ben Gurion University of the Negev, Beer Sheeva 84105, Israel*

(Dated: July 10, 2018)

We develop a microscopic magnetoelectric coupling in $\text{Ni}_3\text{V}_2\text{O}_8$ (NVO) which gives rise to the trilinear phenomenological coupling used previously to explain the phase transition in which magnetic and ferroelectric order parameters appear simultaneously. Using combined neutron scattering measurements and first-principles calculations of the phonons in NVO, we determine eleven phonons which can induce the observed spontaneous polarization. Among these eleven phonons, we find that a few of them can actually induce a significant dipole moment. Using the calculated atomic charges, we find that the required distortion to induce the observed dipole moment is very small (0.001 Å) and therefore it would be very difficult to observe the distortion by neutron-powder diffraction. Finally, we identify the derivatives of the exchange tensor with respect to atomic displacements which are needed for a microscopic model of a spin-phonon coupling in NVO and which we hope will be obtained from a fundamental quantum calculation such as LDA+U. We also analyze two toy models to illustrate that the Dzyaloshinskii-Moriya interaction is very important for coexisting of magnetic and ferroelectric order but it is not the only mechanism when the local site symmetry of the system is low enough.

PACS numbers: 75.25.+z, 75.10.Jm, 75.40.Gb

I. INTRODUCTION

Recently studies have identified a family of multiferroics which display a phase transition in which there simultaneously develops long-range incommensurate magnetic and uniform ferroelectric order. Perhaps the most detailed studies have been carried out on the systems $\text{Ni}_3\text{V}_2\text{O}_8$ (NVO)^{1,2,3,4} and TbMnO_3 (TMO).^{5,6} (For a review, see Ref. 7.) This phenomenon has been explained³ on the basis of a phenomenological model which invokes a Landau expansion in terms of the order parameters describing the incommensurate magnetic order and the order parameter describing the uniform spontaneous polarization. Already from this treatment it was clear that a microscopic model would have to involve a trilinear interaction Hamiltonian proportional to the product of two spin variables and one displacement variable. Furthermore, the symmetry requirements of the phenomenological model would naturally be realized by a proper microscopic model. Accordingly, in this paper we present a detailed combined neutron scattering study and first-principles calculations of the optical phonons of NVO and thereby identify those having the right symmetry to induce a dipole moment. We also consider the expansion of the exchange tensor to first order in the generalized displacement coordinates. The aim of this programme is to determine which of the generalized displacements are relevant and which corresponding elements of the exchange tensor are needed for this microscopic calculation. This paper will therefore set the stage for a separate quantum calculation of the exchange tensor and its derivatives with respect to atomic displacements. On general grounds, one might expect the Dzyaloshinskii-Moriya^{8,9} (DM) in-

teraction to play an important role in this calculation,¹⁰ and indeed, we will find this to be the case. However, the conclusion is a bit more subtle, in that displacement derivatives of many elements of the exchange tensor (and not just the antisymmetric one of the DM interaction) are needed for the microscopic calculation. We will show that simplistic models are somewhat misleading in that they may lead one to believe that the only exchange tensor elements whose derivatives are important are the DM ones. Although our calculations may seem complicated, they are essential if one wishes to actually relate the magnetoelectric coupling to detailed quantum calculations (via LDA¹¹ or LDA+U¹² schemes) of the strain-dependence of the exchange tensors. The methodology of the present paper can be extended in a straightforward way to TMO, for instance.

Briefly this paper is organized as follows. In Sec. II we give an overview of the calculation. In Sec. III we discuss the first-principles calculations of the zone-center phonons and identify those phonons which transform like a vector and which are thus candidates to produce a spontaneous polarization. In this section we also present the neutron scattering measurements of the phonon density of states (DOS), which is found to be in good agreement with the calculated spectrum. Next in Sec. IV we summarize the results of the determination of the spin structure.^{2,4} In Sec. V we then use the symmetry operations of the crystal to show how the phonon derivatives of the various exchange tensors in the unit cell are related to one another. Then in Sec. VI we show that a mean-field treatment of this spin-phonon coupling leads to the results obtained previously^{2,4} in a phenomenological model. Here we give expressions for the spontaneous

polarization in terms of gradients of the exchange tensor whose evaluation remains to be done. It would be nice to have a simple model to illustrate these results. However, our studies of two “toy models” in Sec. VII indicate that they do not reproduce some essential features of our complete calculation. Finally, our conclusions are summarized in Sec. VIII.

II. OVERVIEW OF CALCULATION

Here we give a brief qualitative overview of the calculation. First we review the symmetry of the space group of NVO, Cmca (No. 64 in Ref. 13). The space group operations (apart from primitive translations) are specified in Table I. (Here and below, sites within the unit cell are given as fractions of the sides of the *conventional* unit cell, so that (x, y, z) denotes (xa, yb, zc) .) We now describe the sets of crystallographically equivalent sites which the various atoms occupy. (Such a set of crystallographically equivalent sites is called a *Wyckoff orbit*.) There are six such orbits as shown in Table II. The first two are those of the Ni atoms, the first consisting of the two Ni(1) (a) sites (which we call “cross-tie” sites) and the second consisting of the four Ni(2) (e) sites (which we call “spine” sites). The four V (f) sites comprise the third orbit and the oxygen sites are distributed into two (f) orbits, one containing four O(1) atoms, the other containing four O(2) atoms, and a (g) orbit containing eight O(3) atoms. (The letters a, e, f, g classify the site symmetry according to the convention of Ref. 13. The number of sites in the orbit as listed in Ref. 13 is twice what we give here because here we consider the primitive unit cell rather than the conventional unit cell.) The locations of these sites are specified in the second column of Table II. Note that there are two formula units of NVO per unit cell. The Ni sites form buckled planes which resemble a kagomé lattice and two such adjacent planes are shown in Fig. 1 where the buckling is omitted for simplicity. There one sees that the Ni spine sites form chains along the x -direction between which the Ni cross-tie sites are situated, with bonds to nearest-neighbor spine sites which form a cross tie. To illustrate the use of Table II we find that the eight operations of Table I acting on $(0, 0, 0)$ generate four copies of each of the 2 a sites which are at $(0, 0, 0)$ and $(1/2, 0, 1/2)$. Similarly one can generate the eight g sites by applying in turn the eight operations of Table I to the site at (x, y, z) . (In each case it may be necessary to bring the site back into the original unit cell via a primitive translation vector.)

We now review briefly the nature of the ordered phases which occur as the temperature T is lowered at zero external magnetic field.^{1,2,4} At high temperatures the system is paramagnetic. When T is lowered through the value $T_{PH} \approx 9.1\text{K}$, an incommensurate phase appears (which we call the high-temperature incommensurate or HTI phase) in which the Ni spins on the spine chains are oriented very nearly along the x -axis with a modula-

$\text{Er} = (x, y, z)$	$2_z\mathbf{r} = (\bar{x} + 1/2, \bar{y}, z + 1/2)$
$2_y\mathbf{r} = (\bar{x} + 1/2, y, \bar{z} + 1/2)$	$2_x\mathbf{r} = (x, \bar{y}, \bar{z})$
$\mathcal{I}\mathbf{r} = (\bar{x}, \bar{y}, \bar{z})$	$m_z\mathbf{r} = (x + \frac{1}{2}, y, \bar{z} + \frac{1}{2})$
$m_y\mathbf{r} = (x + \frac{1}{2}, \bar{y}, z + 1/2)$	$m_x\mathbf{r} = (\bar{x}, y, z)$

TABLE I: General positions within the primitive unit cell for Cmca which describe the symmetry operations of this space group. 2_α is a two-fold rotation (or screw) axis and m_α is a mirror (or glide) plane. The primitive translation vectors are $\mathbf{a}_1 = (a/2)\hat{i} + (b/2)\hat{j}$, $\mathbf{a}_2 = (a/2)\hat{i} - (b/2)\hat{j}$, and $\mathbf{a}_3 = c\hat{k}$, where $a = 5.92170\text{\AA}$, $b = 11.37105\text{\AA}$, and $c = 8.22638\text{\AA}$.^{4,14}

Atoms	(x/a,y/b,z/c)	Wyckoff	Decomposition
Ni(1)	(0,0,0)	2a	$A_u + 2B_{1u} + 2B_{2u} + B_{3u}$
Ni(2)	(1/4,y/b,1/4) y=0.1298 (0.1304)	4e	$A_u + 2B_{1u} + B_{2u} + 2B_{3u}$ $A_g + 2B_{1g} + B_{2g} + 2B_{3g}$
V(1)	(0,y,z) y=0.3762 (0.3762) z=0.1197 (0.1196)	4f	$A_u + 2B_{1u} + 2B_{2u} + B_{3u}$ $2A_g + 2B_{1g} + B_{2g} + 2B_{3g}$
O(1)	(0,y/b,z/c) y=0.2481 (0.2490) z=0.2308 (0.2301)	4f	$A_u + 2B_{1u} + 2B_{2u} + B_{3u}$ $2A_g + 2B_{1g} + B_{2g} + 2B_{3g}$
O(2)	(0,y/b,z/c) y=0.0011(0.0008) z=0.2444 (0.2441)	4f	$A_u + 2B_{1u} + 2B_{2u} + B_{3u}$ $2A_g + 2B_{1g} + B_{2g} + 2B_{3g}$
O(3)	(x/a,y/b,z/c) x=0.2656(0.2703) y=0.1192 (0.1184) z=0.0002 (0.0012)	8g	$3A_u + 3B_{1u} + 3B_{2u} + 3B_{3u}$ $3A_g + 3B_{1g} + 3B_{2g} + 3B_{3g}$

TABLE II: In column 2 we give the Wyckoff positions, the fractional coordinates (in column 2) and their multiplicity (in column 3) of atoms in the Wyckoff orbits of NVO listed in column 1. In column 2 we give the values of the structural parameters (e.g. x , y , and z) as deduced from diffraction data^{4,14} and the corresponding values we find from the structural minimization are given in parentheses. In column 4 we give the symmetry decomposition of the displacements of atoms in each of the Wyckoff orbits.

tion vector also along \hat{i} . (The axes are denoted either \mathbf{a} , \mathbf{b} , and \mathbf{c} , or x , y , and z and corresponding unit vectors are denoted \hat{i} , \hat{j} , and \hat{k} .) As the temperature is further lowered through the value $T_{HL} \approx 6.3\text{K}$ transverse order appears at the same incommensurate wavevector and also order appears on the cross-tie sites, as shown in Fig. 1. We call this phase the low-temperature incommensurate or LTI phase. Within experimental uncertainty, these two ordering transitions are continuous. As the temperature is lowered through the value $T_{LC} \approx 4\text{K}$, a discontinuous transition occurs in which a commensurate antiferromagnetic phase appears. In this phase antiferromagnetism results from the arrangement of spins within the unit cell in such a way that the magnetic unit cell remains identical to the paramagnetic unit cell.

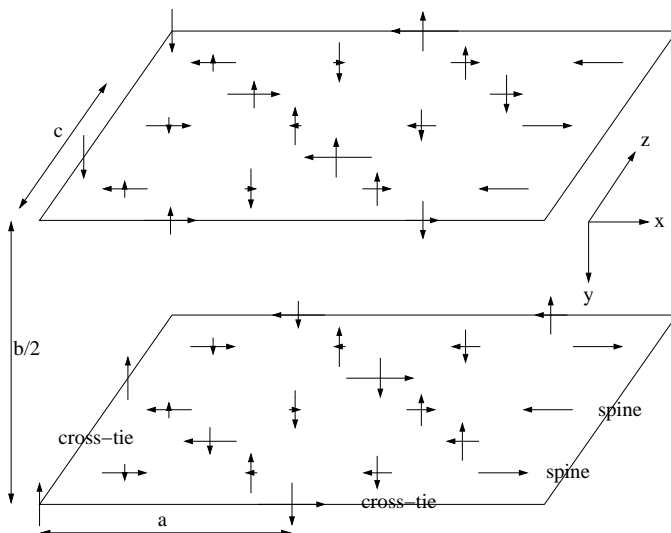


FIG. 1: Schematic diagram showing the x - and y -components of the spins in the LTI phase. We used the parameters: $q = 0.28(2\pi/a)$, $a_{s,x} = 1.6$, $a_{c,y} = 1.4$, $b_{s,y} = 1.3$, $b_{c,x} = -2.2$, and $\phi_L = \phi_H + \pi/2$. The small z -components of spin are not represented. The planes are buckled, so that alternately spine chains are displaced above and below the planes shown (but this buckling is not shown). In the HTI phase the cross-ties have negligible moments and the spine chains have the incommensurately modulated longitudinal moments similar to those shown. The a spin components are odd under 2_x and the b spin components are even under 2_x , where 2_x is a two-fold rotation about the x axis.

Perhaps surprisingly, it was found that ferroelectricity coincides with the existence of LTI order, and this behavior was explained by a phenomenological model based on a Landau expansion in powers of order parameters describing ferroelectricity and those needed to describe the magnetic ordering of the HTI and LTI phases.³ The phenomenological interaction V between the magnetic and ferroelectric order parameters was given as

$$V = \sum_{\alpha} \sum_{X,Y=L,H} a_{\alpha,X,Y} \sigma_X(\mathbf{q}) \sigma_Y(-\mathbf{q}) P_{\alpha}, \quad (1)$$

where $\sigma_X(\mathbf{q})$ is the order parameter describing incommensurate order at wavevector \mathbf{q} characteristic of the HTI phase (for $X=H$) or for the additional ordering appearing in the LTI phase (for $X=L$) and α labels the Cartesian component of the uniform spontaneous polarization vector \mathbf{P} . Using the symmetry properties of the order parameters $\sigma_H(\mathbf{q})$ and $\sigma_L(\mathbf{q})$ it was shown that only $a_{b,L,H}$ and $a_{b,H,L}$ are nonzero. This result provides a phenomenological explanation for the experimental finding that a nonzero polarization is induced by incommensurate magnetism only in the LTI phase and then only with \mathbf{P} along the \mathbf{b} axis.

This phenomenological theory elucidates the symmetry of the magnetically induced ferroelectric state. To develop an analogous microscopic theory, one could treat a Hubbard-like Hamiltonian involving the 3d electrons of

the Ni ions and also the 2p electrons of the O ions. From such a treatment one can obtain the *spin Hamiltonian* which describes the “low energy” sector of this Hubbard-like Hamiltonian. This low-energy sector is obtained by removing states whose energy relative to the low energy sector involves Coulomb integrals. In this approach one develops a canonical transformation to eliminate hopping matrix elements. This approach is obviously most appropriate for insulators. This type of calculation was formalized by Anderson¹⁵ who thereby obtained the antiferromagnetic Heisenberg model from a superexchange mechanism. More recently this approach has been applied to LaCu_2O_4 ^{16,17} and LaTiO_3 .^{18,19} Here we will use the phenomenological model to deduce the form of the low energy spin Hamiltonian which describes magnetically induced ferroelectricity in NVO. We are currently analyzing the more basic Hubbard-like Hamiltonian to show how it gives rise to the spin Hamiltonian.

From the form of Eq. (1), it is clear that the spin-phonon Hamiltonian we seek must be of the form

$$V_{\text{sp-ph}} = \sum_{i,j,k} \sum_{\alpha\beta\gamma} b_{\alpha\beta\gamma k} S_{\alpha}(i) S_{\beta}(j) Q_{\gamma k}, \quad (2)$$

where $\mathbf{S}(i)$ is the vector spin operator for site i and $Q_{\gamma k}$ is the k th normal mode amplitude at zero wavevector which transforms like the γ component of a first rank tensor (vector). We will discuss the normal modes in some detail in the next section. To implement the interaction of Eq. (2) it is convenient to classify both the normal modes and the spin components according to their transformation properties. This interaction represents a linear potential, *i. e.* a force on the phonon coordinate $Q_{\gamma k}$. Up to quadratic order in the displacements the terms in the elastic potential energy V_{el} which depend on the $Q_{\gamma k}$ are

$$V_{\text{el}} = \frac{1}{2} \sum_{\gamma,k} \omega_{\gamma k}^2 Q_{\gamma k}^2 + V_{\text{sp-ph}}. \quad (3)$$

Minimization of this elastic energy with respect to the phonon coordinates leads to a phonon displacement which is proportional to the product of two spin functions, whose symmetry we analyze below. Furthermore, since the displaced ions carry an electric charge (albeit an effective charge), these displacements will give rise to a spontaneous polarization providing the necessary spin components are nonzero. This calculation will recover the symmetry properties of the phenomenological treatment.

III. ZONE-CENTER PHONONS; NEUTRON SCATTERING MEASUREMENTS AND FIRST PRINCIPLES CALCULATIONS

A. Generalized Displacements

Since the normal modes are complicated linear combination of atomic displacements we start by giving a qualitative discussion of generalized displacements (GD's),

	1	2_y	2_x	2_z	\mathcal{I}	m_y	m_x	m_z	Function
A_g	1	1	1	1	1	1	1	1	x^2, y^2, z^2
A_u	1	1	1	1	-1	-1	-1	-1	xyz
B_{2g}	1	1	-1	-1	1	1	-1	-1	xz
B_{2u}	1	1	-1	-1	-1	1	1	1	y
B_{3g}	1	-1	1	-1	1	-1	1	-1	yz
B_{3u}	1	-1	1	-1	-1	1	-1	1	x
B_{1g}	1	-1	-1	1	1	-1	-1	1	xy
B_{1u}	1	-1	-1	1	-1	1	1	-1	z

TABLE III: Irreducible representation of the paramagnetic space group of NVO. The vector representations are B_{1u} , B_{2u} , and B_{3u} which transform like z , y , and x , respectively.

which are linear combinations of atomic displacements which transform according to the various irreducible representations (irreps), whose characters are given in Table III, for the paramagnetic space group of NVO. The actual phonon modes are linear combinations (which we will give later) of these basis functions or GD's.

We are only interested in GD's which transform according to the vector irreps B_{nu} , for $n = 1, 2, 3$. We now give a qualitative discussion of these vector GD's. It is actually quite easy to generate the GD's which transform like vector components x , y , and z . First of all, one sees that assigning all atoms of a given Wykoff orbit the *same* displacement along the α -axis will give a GD which transforms under the symmetry operations of the space group (given in Table I) like the α component of a vector. Since NVO has 6 crystallographically inequivalent sites this construction gives six GD's along each of the three coordinate axes, which we denote x_n , y_n , and z_n , for $n = 1, 2, \dots, 6$. We now discuss the construction of the less trivial GD's which transform like a vector and which are shown in Figs. 2, 3, and 4. To generate these results, one can start with an arbitrarily chosen site to which a vector displacement along one of the three coordinate axes is specified. Then one generates the displacements of the other sites in the Wykoff orbit so as to reproduce the desired transformation properties. For example, to construct a z -like mode on the spines, we could assign the lower left spine site (in the lower left panel of Fig. 2) a displacement along the x -axis. To be a z -like mode the pattern of displacements should be even under m_x , which fixes the displacement of the lower right spine to be that shown. Such a z -like mode should be odd under a two-fold rotation about an x -axis passing through the center of the cell. Applying this operation to the two lower spine sites fixes the orientation of the displacements of the upper spine sites. The other four symmetry operations give these same displacements. Had we started with a spine site with a displacement along the y -axis, we would have gotten a null displacement because this symmetry with displacements along the y -axis is not allowed. Had we fixed the first site to have a displacement along the z -axis we would have found the trivial mode in which

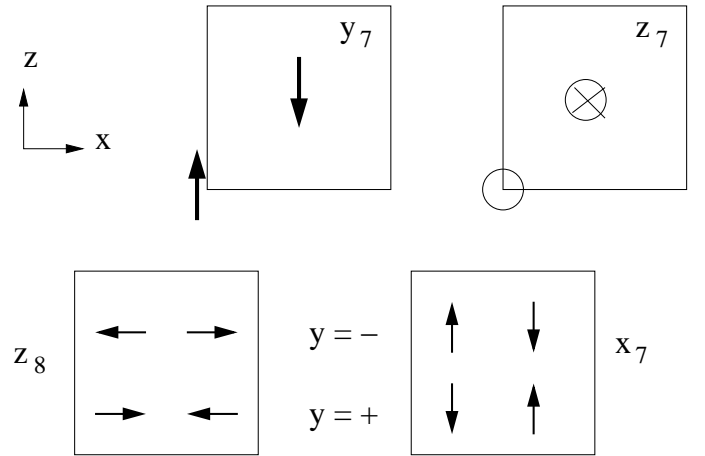


FIG. 2: Generalized displacements y_7 , z_7 , z_8 , and x_7 which transform like the components of a vector, for cross-tie sites (upper panels) and spine sites (lower panels). Atomic displacements (for the GD's indicated by the labels) in the x - z plane are represented by arrows, whereas those in the $+y$ direction ($-y$ direction) are indicated by filled (open) circles. It is easy to see that these modes couple to the uniform displacements. For instance, consider the mode z_8 shown here and in particular consider how the ionic displacements of the spine sites which are shown affect the cross-tie sites (not shown) at the corners and centers of the square. Imagine the ion-ion interactions to be repulsive. Then the nearest neighbors at negative z relative to each cross-tie get closer to the cross-tie and the nearest neighbors at positive z relative to each cross-tie get farther away from the cross-tie. Thus, all cross-ties are squeezed towards positive z . This same reasoning also shows that even though this motion is confined to the x -direction, it will induce a dipole moment along the z -direction.

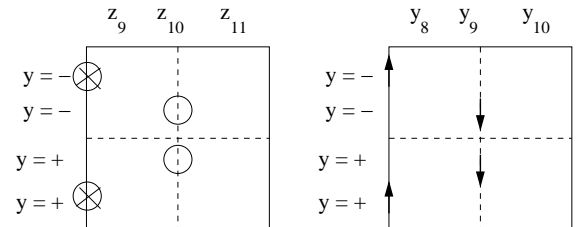


FIG. 3: As Fig. 2. Here we illustrate schematically the vector GD's z_9 , z_{10} , z_{11} , y_8 , y_9 , and y_{10} for f sites. The placement of the sites reproduces the symmetry of an f site and is not quantitative for either V or O atoms. Three distinct f sites are occupied, one by a V atom and the other two by O atoms.

all sites are displaced in parallel. The other GD's shown in the figures were generated in this way. Of course, the actual normal modes (phonons) consist of linear combinations of basis functions having the same irrep label and they will be discussed in the next subsection.

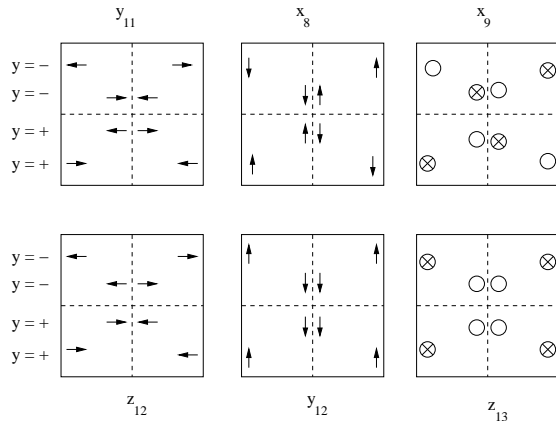


FIG. 4: As Fig. 3. Here we illustrate schematically the vector GD's y_{11} , x_8 , x_9 , z_{12} , y_{12} , and z_{13} for g sites.

B. Normal Modes

In this section we present inelastic neutron scattering (INS) measurements of the phonon density of states (DOS) in NVO along with the first-principles calculations of the zone-center phonons. We will identify the phonons which have the correct symmetry to induce a spontaneous polarization. We will also attempt to estimate the local distortion which gives rise to the observed dipole moment in NVO.

The INS measurements were performed using the filter analyzer spectrometer (FANS) located on beamline BT4 at the NIST Center for Neutron Research²⁰. For energies above 40 meV, a Cu(220) monochromator, surrounded by 60'–40' horizontal collimation and combined with a cooled polycrystalline beryllium filter analyzer was used. For the low energy spectrum (i.e. $E < 40$ meV), a graphite (PG) monochromator with 20'–20' collimation was used. The relative energy resolution of the FANS instrument is approximately 5% in the energy range probed. The powder $\text{Ni}_3\text{V}_2\text{O}_8$ sample (about 20 grams) was held at 12 K (paramagnetic phase) and 8 K (HTI phase) with a helium-filled aluminum can using a closed-cycle He^3 refrigerator.

The first-principles total-energy and phonon calculations were performed by the plane-wave implementation of the spin-polarized generalized gradient approximation (SP-GGA) to density functional theory (DFT).²¹ We used $4 \times 4 \times 3$ k-points according to Monkhorst-pack scheme and Vanderbilt ultra-soft pseudopotentials for which a cutoff energy of 400 eV was found to be enough for total energies to converge within 0.5 eV/atom. We considered the primitive unit cell of the NVO which contains 26 atoms as listed in Table II. Experimental lattice parameters were used in the calculations but the atomic positions were optimized to eliminate the forces down to 0.02 eV/Å. The optimized positions are listed in Table. II, which are in excellent agreement with the experimental positions. Using the optimized structure, we next

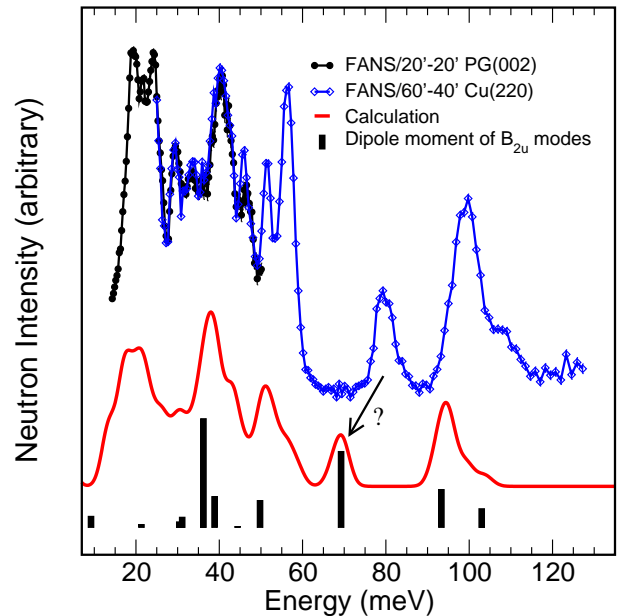


FIG. 5: The observed and calculated INS spectrum. The black vertical bars show the B_{2u} phonons whose intensity is proportional to the induced dipole moment when the system is distorted by the zero-point rms values of the modes.

calculated the zone-center phonons and the corresponding INS one-phonon spectrum as described in Ref. 22.

The measured INS spectrum along with the calculation is shown in Fig. 5. We observed almost identical spectra in the paramagnetic ($T = 12$ K) and the HTI ($T = 8$ K) phases and therefore show only the combined spectrum. The agreement of the calculations to the observed spectrum is quite good, giving further confidence that the first-principle calculations capture the main physics. It also suggests that the phonon modes in NVO have small dispersion with wavevector. This is because the INS spectrum is approximately averaged over a large range of \mathbf{Q} and the calculations are only for $Q = 0$. The biggest difference between the INS spectrum and calculation is for the observed feature near 80 meV, which is calculated to be around 70 meV. As we discuss in detail below, interestingly this phonon has the right symmetry and the atomic displacement vector to induce a large dipole moment. Hence, maybe the disagreement for the energy of this mode could be some indication of strong spin-phonon coupling.

In order to identify the right phonon modes that can induce the observed dipole moment along the \mathbf{b} -axis in NVO, we carried out the symmetry analysis of the zone center phonons. Table III shows the character table for the irreducible representations (irreps) of the group $G_{\mathbf{v}}$ for optical phonons at zero wavevector \mathbf{v} . (For a review of group theory see Ref. 24.) There are 26 atoms in the primitive unit cell and the representation Γ_u induced by the vector space of these $26 \times 3 = 78$ atomic displacements

has the decomposition

$$\Gamma_u = 10A_g + 8A_u + 8B_{1g} + 13B_{1u} + 7B_{2g} + 12B_{2u} + 11B_{3g} + 9B_{3u} . \quad (4)$$

One can check that the vector representations which transform like x , y , and z are B_{3u} , B_{2u} , and B_{1u} , respectively. To discuss the spontaneous polarization these are the only irreps we will need to consider. Among the 78 phonons, twelve have B_{2u} symmetry, and can therefore produce the observed³ spontaneous polarization along the \mathbf{b} -axis. One of these twelve modes is acoustic (i.e. all atoms move uniformly along the \mathbf{b} -axis) and will not be considered any further. To calculate the phonon energies and wavefunctions we found the eigenvalues ω_n^2 of the matrix $\mathbf{W}(q=0)$, which is related to the Fourier transform of the potential energy matrix by $W_{\tau,\alpha;\tau',\alpha'}(q=0) = \sqrt{M_\tau}V_{\tau,\alpha;\tau',\alpha'}(q=0)\sqrt{M_{\tau'}}$, where τ labels sites within the primitive unit cell, α labels Cartesian components, and M_τ is the mass of the atom at site τ . The corresponding eigenvectors $O_{\tau,\alpha}^{(n)}$ are given in Table IV. Thus the displacements within the unit cell are given in terms of the normal modes operators Q_n as

$$\begin{aligned} u_{\tau,\alpha} &= \sum_n O_{\tau,\alpha}^{(n)} M_\tau^{-1/2} Q_n \\ &= \sum_n O_{\tau,\alpha}^{(n)} \sqrt{\frac{\hbar}{2M_\tau\omega_n}} (a_n^\dagger + a_n) , \end{aligned} \quad (5)$$

where a_n^\dagger is a phonon creation operator. The energies of the eleven optical modes are shown in Fig. 5 by black bars whose height for mode n is proportional to the average polarization $\mathbf{P}_y^{(n)}$ of that mode along the y axis. The polarization vector of the n th mode is estimated from the following formula:

$$P_{\text{rms},\alpha}^{(n)} = \frac{1}{\Omega_{\text{uc}}} \sum_\tau q_\tau O_{\tau,\alpha}^{(n)} Q_{\text{rms}} M_\tau^{-1/2} , \quad (6)$$

where Ω_{uc} is the volume of the unit cell and $Q_{\text{rms}} = \sqrt{\hbar/2\omega}$ is the average zero-point fluctuation. As we can see from Fig. 5, half of the B_{2u} modes induce relatively small dipole moments. This is due to the fact that for these phonons, atoms mainly oscillate along the \mathbf{c} -axis and the b -component of the motion is only a second order effect. However for the other half, the motion is directly along the \mathbf{b} -axis and therefore the induced dipole moment is significant. Animations of these modes and more information can be obtained at Ref. 23. We note that two particular phonons, one at 36 meV and the other around 70 meV, induce a significantly large dipole moment. The eigenvectors of these and the other B_{2u} modes along with the magnitude of the induced dipole moments are given in Table IV.

Figure 6 shows schematically how the oxygen atoms move in these two particularly interesting phonons. For the low-energy mode at 36 meV, the two oxygen atoms connecting the spine-spins move in the same direction.

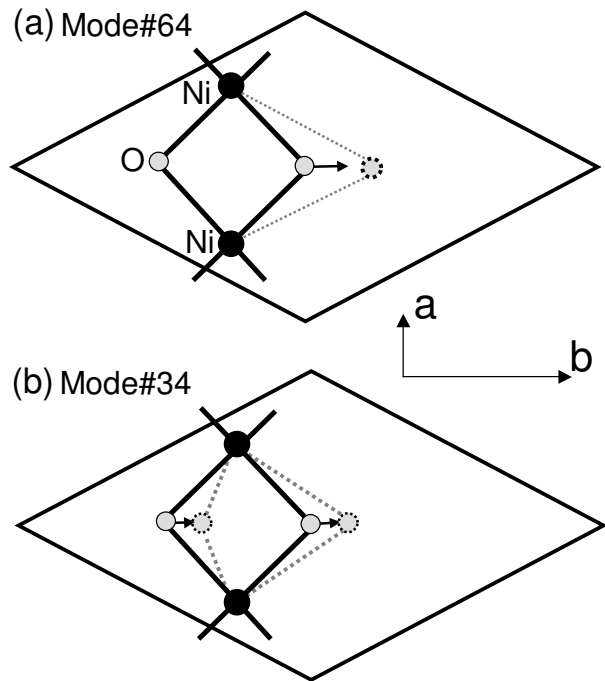


FIG. 6: A schematic representation of the top view of two particularly interesting B_{2u} modes whose displacement vectors are given in Table IV.

Therefore while one of the Ni-O-Ni bond angle decreases, the other Ni-O-Ni bond angle increases. Hence at first order, we do not expect large changes in the Ni-O-Ni superexchange due to this phonon. On the other hand, for the $E = 70$ meV mode, only one oxygen (which is connected to the cross-tie Ni spin) moves along the \mathbf{b} -axis. Hence, in this case, only one of the Ni-O-Ni bond angles changes from nearly 90° and therefore we expect this phonon to have important effects on the Ni-O-Ni superexchange interaction. Interestingly, the biggest disagreement between the experimental data and the calculated phonon energies happens for this phonon, which further suggests that it may have strong spin-phonon coupling.

Finally, we discuss what kind of distortion is needed in order to induce the experimentally observed dipole moment whose magnitude is about $P_{\text{exp}} = 1.25 \times 10^{-4}$ C/m². We note that this induced dipole moment is much smaller than the calculated rms dipole moment ($P_{\text{rms}} \sim 46 - 70 \times 10^{-4}$ C/m²) listed in Table IV. This suggests that the local distortion should be at the order of $P_{\text{exp}}/P_{\text{rms}}$, which suggests that atoms move less than 0.001 Å. This is a quite small distortion and would be very difficult to observe directly by neutron powder diffraction.

	Ni(1) $q = 0.90e$	Ni(2) $q = 0.86e$	V(1) $q = 1.18e$	O(1) $q = -0.62e$	O(2) $q = -0.68e$	O(3) $q = -0.59e$	ω (meV)	$\frac{Q_{rms}}{\sqrt{m_p}}$ (Å)	P_{rms} (10^{-4} C/m ²)
Mode	(0, y , z) y z	(0, y , 0) y	(0, y , z) y z	(0, y , z) y z	(0, y , z) y z	(x , y , z) x y z			
#4	0.023 -0.446	-0.119	0.040 0.169	-0.032 -0.015	0.025 -0.314	-0.024 0.005 0.048	9.2	0.47	2.5
#16	0.551 -0.007	-0.209	-0.094 -0.063	-0.099 -0.111	-0.061 0.069	0.013 0.073 -0.001	21.3	0.31	1.7
#27	-0.205 0.058	-0.110	0.206 0.172	-0.006 -0.354	0.023 -0.061	0.071 0.041 0.009	30.4	0.26	3.3
#29	-0.008 -0.428	0.019	0.010 -0.265	0.090 0.050	-0.053 0.086	-0.020 -0.040 -0.178	31.1	0.26	6.1
#34	-0.164 0.066	-0.286	0.073 0.049	0.109 0.163	0.103 0.077	-0.073 0.188 -0.068	36.2	0.24	66.1
#40	0.178 0.113	-0.166	0.162 -0.012	0.157 0.076	0.171 -0.012	0.029 -0.237 0.007	38.9	0.23	18.7
#49	0.069 0.307	0.021	-0.056 -0.138	0.023 0.057	-0.069 -0.348	-0.068 0.015 -0.139	44.4	0.22	0.5
#53	-0.014 -0.022	-0.037	-0.043 0.165	0.143 0.182	-0.112 -0.080	0.212 0.066 0.155	49.8	0.20	16.3
#64	0.037 0.041	-0.030	0.264 0.110	0.015 0.047	-0.396 0.042	-0.038 -0.027 -0.010	69.2	0.17	46.1
#70	0.011 -0.011	0.001	-0.155 0.017	0.365 -0.169	-0.081 0.011	-0.143 -0.004 0.090	93.3	0.15	23.0
#78	0.010 0.019	0.004	-0.089 0.238	0.150 -0.099	-0.029 0.000	0.203 0.009 -0.187	103.0	0.14	11.3

TABLE IV: Mass-weighted atomic displacements of B_{2u} phonons which induce a dipole moment along the \mathbf{b} axis (normalized so that the sum of the squares of the components equals unity for each mode). (The acoustic B_{2u} is not tabulated.) Each component of the mass-weighted displacement represents the atomic displacement divided by the square root of the respective atomic mass. The mass-weighted displacements are given for the sites listed in column #2 of Table II. The displacements of the remaining atoms in each Wyckoff orbit are fixed so that the mode transforms like B_{2u} , i. e. like the y -component of a vector. The calculated atomic charges, magnitude of the rms displacement Q_{rms} (where m_p is the proton mass), the rms dipole moment, and the mode energy is also given.

	1	2_x	\tilde{m}_y	\tilde{m}_z
Γ^1	1	1	1	1
Γ^2	1	1	-1	-1
Γ^3	1	-1	1	-1
Γ^4	1	-1	-1	1

TABLE V: Irreducible representations of the group $G_{\mathbf{v}}$ for the incommensurate magnetic structure with $\mathbf{v} = (q, 0, 0)$. Here it is simplest to use the symmetry operations \tilde{m}_y and \tilde{m}_z , such that $\tilde{m}_y \mathbf{r} = (x, \bar{y} + \frac{1}{2}, z + \frac{1}{2})$ and $\tilde{m}_z \mathbf{r} = (x, y + \frac{1}{2}, \bar{z} + \frac{1}{2})$.

IV. SYMMETRY OF THE SPIN STRUCTURE

In Refs. 3, 4, 7, and 25 the application of representation theory to the determination and characterization of magnetic structures is discussed in detail. In Table V we give the character table for the irreps for an arbitrary wavevector of the form $(q, 0, 0)$. Because the irreps are one dimensional, each spin basis function is an eigenvector of the symmetry operator with the listed eigenvalue.

In these references it is shown that the HTI phase is described by a set of five complex amplitudes associated with the irrep Γ_4 . Here we call these $a_{s,x}$, $ia_{s,y}$, and $a_{s,z}$ to describe the orientation of the spine spins and $a_{c,y}$ and $a_{c,z}$ to describe the orientation of the cross-tie spins. When the LTI phase is entered additional variables associated with the irrep Γ_2 become nonzero. These LTI variables are here denoted $ib_{s,x}$, $b_{s,y}$, and $ib_{s,z}$ to describe the orientation of the spine spins and $b_{c,z}$ to describe the orientation of the cross tie spins. Because the crystal is

centrosymmetric, it is shown^{4,7,25} that within a given representation all these complex structural parameters (the a 's and b 's) can be written in terms of a real amplitude times a complex phase factor which is the same for all variables of the same irrep, Γ_4 or Γ_2 , in the sense that

$$a_{t,\alpha} = \pm |a_{t,\alpha}| e^{i\phi_{HTI}}, \quad b_{t,\alpha} = \pm |b_{t,\alpha}| e^{i\phi_{LTI}}, \quad (7)$$

where t denotes either spine or cross-tie. It is further expected^{4,25} that $\phi_{HTI} - \phi_{LTI}$ is $\pm\pi/2$. Thus in these two phases we may use the results of Table VIII in Ref. 4 to write the spin components of the six Ni ions in the unit cell as

$$S_x^{(1)}(\mathbf{R}_1) = (a_{s,x} + ib_{s,x})e^{i\mathbf{q}\cdot\mathbf{R}_1} + (a_{s,x}^* - ib_{s,x}^*)e^{-i\mathbf{q}\cdot\mathbf{R}_1} \quad (8)$$

$$S_y^{(1)}(\mathbf{R}_1) = (ia_{s,y} + b_{s,y})e^{i\mathbf{q}\cdot\mathbf{R}_1} + (-ia_{s,y}^* + b_{s,y}^*)e^{-i\mathbf{q}\cdot\mathbf{R}_1} \quad (9)$$

$$S_z^{(1)}(\mathbf{R}_1) = (a_{s,z} + ib_{s,z})e^{i\mathbf{q}\cdot\mathbf{R}_1} + (a_{s,z}^* - ib_{s,z}^*)e^{-i\mathbf{q}\cdot\mathbf{R}_1} \quad (10)$$

$$S_x^{(2)}(\mathbf{R}_2) = (-a_{s,x} + ib_{s,x})e^{i\mathbf{q}\cdot\mathbf{R}_2} + (-a_{s,x}^* - ib_{s,x}^*)e^{-i\mathbf{q}\cdot\mathbf{R}_2} \quad (11)$$

$$S_y^{(2)}(\mathbf{R}_2) = (ia_{s,y} - b_{s,y})e^{i\mathbf{q}\cdot\mathbf{R}_2} + (-ia_{s,y}^* - b_{s,y}^*)e^{-i\mathbf{q}\cdot\mathbf{R}_2} \quad (12)$$

$$S_z^{(2)}(\mathbf{R}_2) = (a_{s,z} - ib_{s,z})e^{i\mathbf{q}\cdot\mathbf{R}_2} + (a_{s,z}^* + ib_{s,z}^*)e^{-i\mathbf{q}\cdot\mathbf{R}_2} \quad (13)$$

$$S_x^{(3)}(\mathbf{R}_3) = (a_{s,x} - ib_{s,x})e^{i\mathbf{q}\cdot\mathbf{R}_3}$$

$$+(a_{s,x}^* + ib_{s,x}^*)e^{-i\mathbf{q}\cdot\mathbf{R}_3} \quad (14)$$

$$S_y^{(3)}(\mathbf{R}_3) = (-ia_{s,y} + b_{s,y})e^{i\mathbf{q}\cdot\mathbf{R}_3} \\ + (ia_{s,y}^* + b_{s,y}^*)e^{-i\mathbf{q}\cdot\mathbf{R}_3} \quad (15)$$

$$S_z^{(3)}(\mathbf{R}_3) = (a_{s,z} - ib_{s,z})e^{i\mathbf{q}\cdot\mathbf{R}_3} \\ + (a_{s,z}^* + ib_{s,z}^*)e^{-i\mathbf{q}\cdot\mathbf{R}_3} \quad (16)$$

$$S_x^{(4)}(\mathbf{R}_4) = (-a_{s,x} - ib_{s,x})e^{i\mathbf{q}\cdot\mathbf{R}_4} \\ + (-a_{s,x}^* + ib_{s,x}^*)e^{-i\mathbf{q}\cdot\mathbf{R}_4} \quad (17)$$

$$S_y^{(4)}(\mathbf{R}_4) = (-ia_{s,y} - b_{s,y})e^{i\mathbf{q}\cdot\mathbf{R}_4} \\ + (ia_{s,y}^* - b_{s,y}^*)e^{-i\mathbf{q}\cdot\mathbf{R}_4} \quad (18)$$

$$S_z^{(4)}(\mathbf{R}_4) = (a_{s,z} + ib_{s,z})e^{i\mathbf{q}\cdot\mathbf{R}_4} \\ + (a_{s,z}^* - ib_{s,z}^*)e^{-i\mathbf{q}\cdot\mathbf{R}_4} \quad (19)$$

$$S_x^{(5)}(\mathbf{R}_5) = b_{c,x}e^{i\mathbf{q}\cdot\mathbf{R}_5} + b_{c,x}^*e^{-i\mathbf{q}\cdot\mathbf{R}_5} \quad (20)$$

$$S_y^{(5)}(\mathbf{R}_5) = a_{c,y}e^{i\mathbf{q}\cdot\mathbf{R}_5} + a_{c,y}^*e^{-i\mathbf{q}\cdot\mathbf{R}_5} \quad (21)$$

$$S_z^{(5)}(\mathbf{R}_5) = a_{c,z}e^{i\mathbf{q}\cdot\mathbf{R}_5} + a_{c,z}^*e^{-i\mathbf{q}\cdot\mathbf{R}_5} \quad (22)$$

$$S_x^{(6)}(\mathbf{R}_6) = -b_{c,x}e^{i\mathbf{q}\cdot\mathbf{R}_6} - b_{c,x}^*e^{-i\mathbf{q}\cdot\mathbf{R}_6} \quad (23)$$

$$S_y^{(6)}(\mathbf{R}_6) = -a_{c,y}e^{i\mathbf{q}\cdot\mathbf{R}_6} - a_{c,y}^*e^{-i\mathbf{q}\cdot\mathbf{R}_6} \quad (24)$$

$$S_z^{(6)}(\mathbf{R}_6) = a_{c,z}e^{i\mathbf{q}\cdot\mathbf{R}_6} + a_{c,z}^*e^{-i\mathbf{q}\cdot\mathbf{R}_6} . \quad (25)$$

Here the superscripts on 1, 2, 3, 4 on \mathbf{S} label the spine sites and 5 and 6 label the cross-tie sites c and c' , respectively, (as in Fig. 7, below) and \mathbf{R}_n is the position of a spin n . Also $\mathbf{q} = q\hat{i}$ with $q \approx 0.28(2\pi/a)$.^{2,4}

V. RELATIONS FOR THE STRAIN DERIVATIVE OF THE EXCHANGE TENSOR

In this section we obtain explicit forms for the most important spin-phonon coupling matrices. For this purpose we start by introducing notation for the principal exchange interactions. We write the interactions between spins on sites i and j as

$$\mathcal{H}(i, j) = \sum_{\alpha\beta} X_{\alpha\beta}(i, j)S_\alpha(i)S_\beta(j) , \quad (26)$$

where $X_{\alpha\beta}(i, j) = X_{\beta\alpha}(j, i)$, of course. For nearest neighbor (nn) interactions between spine spins we set $X_{\alpha\beta}(i, j) = U_{\alpha\beta}(i, j)$, for next nearest neighbor (nnn) interactions between spine spins we set $X_{\alpha\beta}(i, j) = V_{\alpha\beta}(i, j)$, and for nn interactions between spine and cross-tie spins we set $X_{\alpha\beta}(i, j) = W_{\alpha\beta}(i, j)$. We may further decompose the exchange tensor into its symmetric and antisymmetric parts. For example, for nn spine-spine interactions we write (omitting the site labels i and j)

$$\mathbf{U} = \begin{bmatrix} J_{xx} & J_{xy} + D_z & J_{xz} - D_y \\ J_{xy} - D_z & J_{yy} & J_{yz} + D_x \\ J_{xz} + D_y & J_{yz} - D_x & J_{zz} \end{bmatrix} , \quad (27)$$

where \mathbf{D} is the Dzyaloshinskii-Moriya (DM) vector.^{8,9} Similar decompositions will be made for \mathbf{V} and \mathbf{W} in

terms of symmetric tensors \mathbf{K} and \mathbf{L} , respectively, and the DM vectors \mathbf{E} and \mathbf{F} , respectively.

Now we consider the gradient expansion of these exchange tensors. From the above development we write the displacement \mathbf{u} of the τ th atom in the unit cell in terms of the amplitude Q_{γ_p} of the GD labeled γ_p as

$$u_\alpha(\mathbf{R}, \tau; \gamma_p) = Q_{\gamma_p}a(\gamma_p; \tau, \alpha) , \quad (28)$$

where $a(\gamma_p; \tau, \alpha)$ is the α -component of the displacement of atom τ in unit cell at \mathbf{R} for the GD labeled γ_p (which are shown in Figs. 2, 3, and 4). If Z represents a component of an exchange tensor, then we write

$$\frac{\partial Z}{\partial Q_{\gamma_p}} = \sum_{\alpha\mathbf{R}\tau} \frac{\partial Z}{\partial u_\alpha(\mathbf{R}, \tau; \gamma_p)} a(\gamma_p; \tau, \alpha) . \quad (29)$$

The aim of the present paper is to determine which such derivatives are required to completely determine the trilinear spin-phonon coupling. The actual calculation of these coefficients will be undertaken separately. Thus, for each GD γ_p , we consider the interaction

$$\mathcal{H}_{\gamma_p} = Q_{\gamma_p} \sum_{\alpha\beta} \sum_{ij} \frac{\partial X_{\alpha\beta}(i, j)}{\partial Q_{\gamma_p}} S_\alpha(i)S_\beta(j) . \quad (30)$$

Our objective is to express the results for the spontaneous polarization due to the trilinear coupling in terms of the parameters $\partial X_{\alpha\beta}(i, j)/\partial Q_{\gamma_p}$.

Here we analyze the gradients of the nn interactions between spine spins. (Similar analyses of next-nearest neighbor spine interactions and of nn spine-cross tie interactions are given in Appendices.) We introduce the coupling between spine sites #1 and #4 in Fig. 7:

$$\frac{\partial U_{\alpha\beta}(1, 4)}{\partial Q_{\gamma_p}} \equiv U_{\alpha\beta}^{\gamma_p} . \quad (31)$$

Clearly \mathbf{U}^{γ_p} has to be invariant under the symmetry operations of the crystal. But m_x takes the bond in question into itself (and interchanges indices). This indicates that these interaction matrices must satisfy

$$\begin{aligned} \sigma_x \mathbf{U}^{x_p} \sigma_x &= -\tilde{\mathbf{U}}^{x_p} \\ \sigma_x \mathbf{U}^{y_p} \sigma_x &= \tilde{\mathbf{U}}^{y_p} \\ \sigma_x \mathbf{U}^{z_p} \sigma_x &= \tilde{\mathbf{U}}^{z_p} , \end{aligned} \quad (32)$$

where tilde indicates transpose,

$$\sigma_x = \begin{bmatrix} -1 & 0 & 0 \\ 0 & 1 & 0 \\ 0 & 0 & 1 \end{bmatrix} ,$$

and later

$$\sigma_y = \begin{bmatrix} 1 & 0 & 0 \\ 0 & -1 & 0 \\ 0 & 0 & 1 \end{bmatrix} ,$$

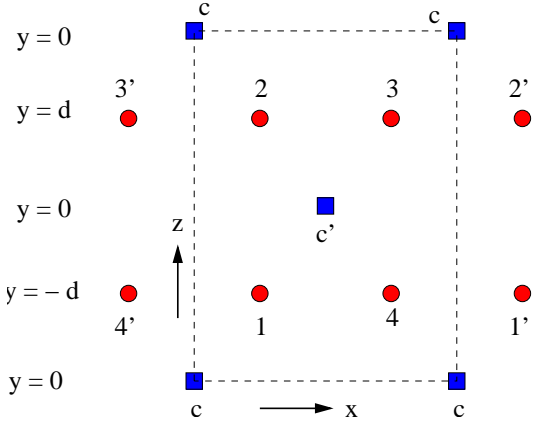


FIG. 7: Diagram of an $a - c$ plane used to specify nearest-neighbor and next-nearest-neighbor interactions along a single spine. Circles are spine sites and square are cross-tie sites and $d = 0.13b$ (see Table II). The dashed rectangle indicates the unit cell. Interactions in other $a - c$ planes are obtained by using translation symmetry.

$$\sigma_z = \begin{bmatrix} 1 & 0 & 0 \\ 0 & 1 & 0 \\ 0 & 0 & -1 \end{bmatrix}. \quad (33)$$

Here we used the fact that the GD's were constructed to have known symmetry:

$$m_\alpha Q_{\beta p} = (1 - 2\delta_{\alpha,\beta})Q_{\beta p} \quad (34)$$

and

$$2_\alpha Q_{\beta p} = (-1 + 2\delta_{\alpha,\beta})Q_{\beta p}, \quad (35)$$

where $\delta_{a,b}$ is unity if $a = b$ and is zero otherwise.

In view of Eq. (32), we have

$$\begin{aligned} \mathbf{U}^{x_p} &= \begin{bmatrix} 0 & J_{xy}^x & J_{xz}^x \\ J_{xy}^x & 0 & D_x^x \\ J_{xz}^x & -D_x^x & 0 \end{bmatrix}, \\ \mathbf{U}^{y_p} &= \begin{bmatrix} J_{xx}^y & D_z^y & -D_y^y \\ -D_z^y & J_{yy}^y & J_{yz}^y \\ D_y^y & J_{yz}^y & J_{zz}^y \end{bmatrix}, \\ \mathbf{U}^{z_p} &= \begin{bmatrix} J_{xx}^z & D_z^z & -D_y^z \\ -D_z^z & J_{yy}^z & J_{yz}^z \\ D_y^z & J_{yz}^z & J_{zz}^z \end{bmatrix}, \end{aligned} \quad (36)$$

where the index p on the superscripts of J and D are left implicit and $J_{\alpha\beta}^{\gamma p}$ and $D_{\alpha}^{\gamma p}$ (and similarly later for superscripts on \mathbf{K} , \mathbf{L} , \mathbf{E} , and \mathbf{F}) are defined to be

$$J_{\alpha\beta}^{\gamma p} \equiv \frac{\partial J_{\alpha\beta}(1,4)}{\partial Q_{\gamma p}}, \quad D_{\alpha}^{\gamma p} \equiv \frac{\partial D_{\alpha}(1,4)}{\partial Q_{\gamma p}}. \quad (37)$$

Then we obtain the #2-#3 interaction from the above by 2_x , a two-fold rotation about the x -axis, so that

$$\frac{\partial U_{\alpha\beta}(2,3)}{\partial Q_{x_p}} = \sigma_y \sigma_z \mathbf{U}^{x_p} \sigma_y \sigma_z$$

$$= \begin{bmatrix} 0 & -J_{xy}^x & -J_{xz}^x \\ -J_{xy}^x & 0 & D_x^x \\ -J_{xz}^x & -D_x^x & 0 \end{bmatrix}, \quad (38)$$

$$\begin{aligned} \frac{\partial U_{\alpha\beta}(2,3)}{\partial Q_{y_p}} &= -\sigma_y \sigma_z \mathbf{U}^{y_p} \sigma_y \sigma_z \\ &= \begin{bmatrix} -J_{xx}^y & D_z^y & -D_y^y \\ -D_z^y & -J_{yy}^y & -J_{yz}^y \\ D_y^y & -J_{yz}^y & -J_{zz}^y \end{bmatrix}, \end{aligned} \quad (39)$$

$$\begin{aligned} \frac{\partial U_{\alpha\beta}(2,3)}{\partial Q_{z_p}} &= -\sigma_y \sigma_z \mathbf{U}^{z_p} \sigma_y \sigma_z \\ &= \begin{bmatrix} -J_{xx}^z & D_z^z & -D_y^z \\ -D_z^z & -J_{yy}^z & -J_{yz}^z \\ D_y^z & -J_{yz}^z & -J_{zz}^z \end{bmatrix}. \end{aligned} \quad (40)$$

where we used Eq. (35).

We obtain the #4-#1' interactions by applying the glide operation m_y to the #2-#3 interaction, so that

$$\begin{aligned} \frac{\partial U_{\alpha\beta}(4,1')}{\partial Q_{x_p}} &= \sigma_y \frac{\partial \mathbf{U}(2,3)}{\partial Q_{x_p}} \sigma_y \\ &= \begin{bmatrix} 0 & J_{xy}^x & -J_{xz}^x \\ J_{xy}^x & 0 & -D_x^x \\ -J_{xz}^x & D_x^x & 0 \end{bmatrix}, \end{aligned} \quad (41)$$

$$\begin{aligned} \frac{\partial U_{\alpha\beta}(4,1')}{\partial Q_{y_p}} &= -\sigma_y \frac{\partial \mathbf{U}(2,3)}{\partial Q_{y_p}} \sigma_y \\ &= \begin{bmatrix} J_{xx}^y & D_z^y & D_y^y \\ -D_z^y & J_{yy}^y & -J_{yz}^y \\ -D_y^y & -J_{yz}^y & J_{zz}^y \end{bmatrix}, \end{aligned} \quad (42)$$

$$\begin{aligned} \frac{\partial U_{\alpha\beta}(4,1')}{\partial Q_{z_p}} &= \sigma_y \frac{\partial \mathbf{U}(2,3)}{\partial Q_{z_p}} \sigma_y \\ &= \begin{bmatrix} -J_{xx}^z & -D_z^z & -D_y^z \\ D_z^z & -J_{yy}^z & J_{yz}^z \\ D_y^z & J_{yz}^z & -J_{zz}^z \end{bmatrix}, \end{aligned} \quad (43)$$

and finally we get the #3-#2' interaction by applying a two-fold rotation about the x -axis to the #4-#1' interaction to get

$$\begin{aligned} \frac{\partial U_{\alpha\beta}(3,2')}{\partial Q_{x_p}} &= \sigma_y \sigma_z \frac{\partial \mathbf{U}(4,1')}{\partial Q_{x_p}} \sigma_y \sigma_z \\ &= \begin{bmatrix} 0 & -J_{xy}^x & J_{xz}^x \\ -J_{xy}^x & 0 & -D_x^x \\ J_{xz}^x & D_x^x & 0 \end{bmatrix}, \end{aligned} \quad (44)$$

$$\begin{aligned} \frac{\partial U_{\alpha\beta}(3,2')}{\partial Q_{y_p}} &= -\sigma_y \sigma_z \frac{\partial \mathbf{U}(4,1')}{\partial Q_{y_p}} \sigma_y \sigma_z \\ &= \begin{bmatrix} -J_{xx}^y & D_z^y & D_y^y \\ -D_z^y & -J_{yy}^y & J_{yz}^y \\ -D_y^y & J_{yz}^y & -J_{zz}^y \end{bmatrix}, \end{aligned} \quad (45)$$

and

$$\begin{aligned} \frac{\partial U_{\alpha\beta}(3,2')}{\partial Q_{z_p}} &= -\sigma_y \sigma_z \frac{\partial \mathbf{U}(4,1')}{\partial Q_{z_p}} \sigma_y \sigma_z \\ &= \begin{bmatrix} J_{xx}^z & -D_z^z & -D_y^z \\ D_z^z & J_{yy}^z & -J_{yz}^z \\ D_y^z & -J_{yz}^z & J_{zz}^z \end{bmatrix}. \end{aligned} \quad (46)$$

VI. MEAN FIELD SPIN-PHONON HAMILTONIAN

A. Mean Field Results

Here we treat the nn spine-spine interactions in detail. Analogous calculations for the nnn spine-spine and nn spine-cross tie interactions are treated in an Appendix. We evaluate the spin-phonon Hamiltonian \mathcal{H}_{γ_p} of Eq. (30) at the mean-field level. In other words, for the spin operators we simply substitute their average values as given in Eqs. (8)-(25). One sees that \mathcal{H}_{x_p} for nn spine-spine interactions, for instance, will consist of contributions proportional to $J_{xy}^{x_p}$, to $J_{xz}^{x_p}$, and to $D_x^{x_p}$. To illustrate the calculation we will explicitly evaluate the first of these, which we denote $\mathcal{H}_{x_p}(J_{xy})$:

$$\begin{aligned} \mathcal{H}_{x_p}(J_{xy}) &= Q_{x_p} J_{xy}^{x_p} \sum_{uc} \left[S_x^{(1)} S_y^{(4)} + S_y^{(1)} S_x^{(4)} \right. \\ &\quad - S_x^{(2)} S_y^{(3)} - S_x^{(3)} S_y^{(2)} + S_x^{(4)} S_y^{(1')} \\ &\quad \left. + S_x^{(1')} S_y^{(4)} - S_x^{(3)} S_y^{(2')} - S_x^{(2')} S_y^{(3)} \right] \end{aligned} \quad (47)$$

where, since we included all interactions within a single unit cell, the sum is over all N_{uc} unit cells. (In this summation only terms involving both \mathbf{q} and $-\mathbf{q}$ survive.) Thus

$$\begin{aligned} \mathcal{H}_{x_p}(J_{xy}) &= 2N_{uc} Q_{x_p} J_{xy}^{x_p} e^{-iqa/2} \\ &\quad \times [(a_{s,x} + ib_{s,x})(ia_{s,y}^* - b_{s,y}^*) \\ &\quad + (ia_{s,y} + b_{s,y})(-a_{s,x}^* + ib_{s,x}^*) \\ &\quad - (-a_{s,x} + ib_{s,x})(ia_{s,y}^* + b_{s,y}^*) \\ &\quad - (ia_{s,y} - b_{s,y})(a_{s,x}^* + ib_{s,x}^*)] + \text{c. c.} \\ &= 16N_{uc} Q_{x_p} J_{xy}^{x_p} \cos(qa/2) \\ &\quad \times \Im[a_{s,x}^* a_{s,y} + b_{s,x} b_{s,y}^*]. \end{aligned} \quad (48)$$

The other terms proportional to Q_{x_p} are

$$\begin{aligned} \mathcal{H}_{x_p}(J_{xz}) &= 16N_{uc} Q_{x_p} J_{xz}^{x_p} \sin(qa/2) \\ &\quad \times \Im[a_{s,x} a_{s,z}^* + b_{s,x} b_{s,z}^*]. \end{aligned} \quad (49)$$

$$\begin{aligned} \mathcal{H}_{x_p}(D_x) &= 16N_{uc} Q_{x_p} D_x^{x_p} \cos(qa/2) \\ &\quad \times \Im[-a_{s,y} a_{s,z}^* + b_{s,y} b_{s,z}^*]. \end{aligned} \quad (50)$$

In view of Eq. (7) all these terms involving Q_{x_p} vanish, as was found from the phenomenological formulation. Similarly, all the terms involving Q_{z_p} also vanish, again in conformity with the phenomenological argument.

We are thus only left with terms involving Q_{y_p} . In Appendix C we find that the strain dependence of the nn spine interactions give

$$\mathcal{H}_{y_p} = 16N_{uc} Q_{y_p} \sum_{\mu,\nu=x,y,z} \Lambda_{\mu\nu}^{(nn)} \Im[a_{s,\mu}^* b_{s,\nu}], \quad (51)$$

where

$$\Lambda^{(nn)} = \begin{bmatrix} J_{xx}^{y_p} c & D_z^{y_p} s & D_y^{y_p} c \\ -D_z^{y_p} s & -J_{yy}^{y_p} c & -J_{yz}^{y_p} s \\ D_y^{y_p} c & J_{yz}^{y_p} s & -J_{zz}^{y_p} c \end{bmatrix}, \quad (52)$$

where $c \equiv \cos(qa/2)$ and $s \equiv \sin(qa/2)$. Using the results of Appendix C we find that the nnn interactions give a result of the form of Eq. (51) but with

$$\Lambda^{(nnn)} = \begin{bmatrix} -K_{xx}^{y_p} c' & -E_z^{y_p} s' & -K_{xz}^{y_p} c' \\ E_z^{y_p} s' & K_{yy}^{y_p} c' & -E_x^{y_p} s' \\ -K_{xz}^{y_p} c' & E_x^{y_p} s' & -K_{zz}^{y_p} c' \end{bmatrix}, \quad (53)$$

where $c' \equiv \cos(qa)$ and $s' \equiv \sin(qa)$. Using the results of Appendix C we have the results for the spine-cross tie exchange gradients:

$$\begin{aligned} V_{y_p} &= 16N_{uc} Q_{y_p} \left(\sum_{\alpha=y,z} \sum_{\beta} \Lambda_{\alpha\beta}^{sx} \Im[a_{c\alpha} b_{s\beta}^*] \right. \\ &\quad \left. + \sum_{\alpha=x} \sum_{\beta} \Lambda_{\alpha\beta}^{sx} \Im[b_{c\alpha} a_{s,\beta}^*] \right), \end{aligned} \quad (54)$$

where Λ^{sx} is

$$\begin{bmatrix} L_{xx}^{y_p} s'' & [L_{xy}^{y_p} + F_z^{y_p}] c'' & [L_{xz}^{y_p} - F_y^{y_p}] s'' \\ [L_{xy}^{y_p} - F_z^{y_p}] c'' & L_{yy}^{y_p} s'' & [L_{yz}^{y_p} + F_x^{y_p}] c'' \\ [L_{xz}^{y_p} + F_y^{y_p}] c'' & [L_{yz}^{y_p} - F_x^{y_p}] s'' & L_{zz}^{y_p} c'' \end{bmatrix} \quad (55)$$

where $c'' \equiv \cos(qa/4)$ and $s'' \equiv \sin(qa/4)$. These results agree with the phenomenological model, in that V_{y_p} is only nonzero when both the “a” and the “b” irreps are simultaneously present and they can not have the same phase (lest a^*b be real).

B. Summary

Here we show how the above results lead to an evaluation of the spontaneous polarization. If we combine the results of Eqs. (51), (53), and (54), we may write

$$V_{y_p} = N_{uc} Q_{y_p} \lambda_{y_p}, \quad p = 1, 12. \quad (56)$$

But the GD's are related to the normal modes via

$$Q_{y_p} = \sum_{n=1,11} o_{y_p}^{(n)} M_p^{-1/2} Q_n, \quad (57)$$

where the orthogonal transformation \mathbf{o} is essentially that given in Table IV apart from normalization factors due to replacing a Wyckoff orbit by one of its atoms. Note that the GD y_p is associated with atoms all having the same mass M_p . The magnetoelectric trilinear interaction in terms of normal mode operators is thus

$$V = N_{uc} \sum_{n,p} \lambda_{y_p} o_{y_p}^{(n)} M_p^{-1/2} Q_n, \quad (58)$$

Since the unperturbed elastic energy is $\mathcal{H}_0 = (N_{uc}/2) \sum_n \omega_n^2 Q_n^2$, we see that the trilinear interaction induces the displacements

$$\langle Q_n \rangle = \sum_p \lambda_{y_p} o_{y_p}^{(n)} M_p^{-1/2} \omega_n^{-2}, \quad (59)$$

from which we obtain the induced spontaneous polarization as

$$P_y = \frac{1}{\Omega_{uc}} \sum_{n,p} q_p o_{y_p}^{(n)} \langle Q_n \rangle M_p^{-1/2}, \quad (60)$$

where the atomic charges q_p are given in Table IV. The only ingredients we do not have for this evaluation are the various gradients of the exchange tensors.

VII. TOY MODELS

In this section we will consider two toy models. In the first one, we consider a single spine with one Ni per unit cell, but with two oxygen atoms symmetrically placed on either side of the spine. In this version, all atoms lie in a single plane. In the second version, the size of the unit cell is doubled. In one plaquette the oxygen atoms are both displaced equally perpendicularly to the original atomic plane and in the next plaquette the oxygens are oppositely displaced. In this version one of the mirror planes becomes a glide plane. These models illustrate the simplifications which arise when the system has higher symmetry than the buckled kagomé lattice of NVO.

A. Unit cell with two atoms

In this section we consider the toy model shown in the left panel of Fig. 8. We first analyze the symmetry of the strain derivatives of the exchange tensor. By translational symmetry all nearest neighbor interactions are equivalent. So we set

$$\frac{\partial J_{\alpha\beta}(n, n+1)}{\partial Q_{\gamma_p}} \equiv \mathbf{J}_{\alpha\beta}^{\gamma_p} = \begin{bmatrix} J_{xx}^{\gamma} & J_{xy}^{\gamma} + D_z^{\gamma} & J_{xz}^{\gamma} - D_y^{\gamma} \\ J_{xy}^{\gamma} - D_z^{\gamma} & J_{yy}^{\gamma} & J_{yz}^{\gamma} + D_x^{\gamma} \\ J_{xz}^{\gamma} + D_y^{\gamma} & J_{yz}^{\gamma} - D_x^{\gamma} & J_{zz}^{\gamma} \end{bmatrix}, \quad (61)$$

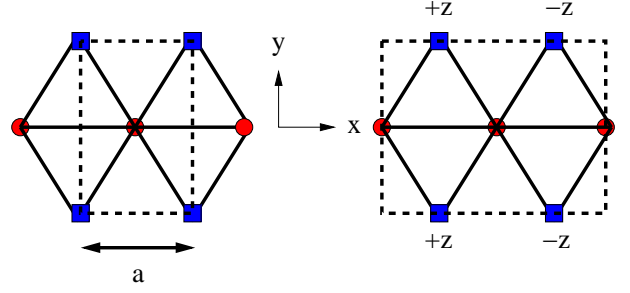


FIG. 8: The two toy models. In each case the unit cell is bounded by a dashed line. The filled circles are Ni sites and the squares are O sites.

where $J_{\alpha\beta}^{\gamma} \equiv \partial J_{\alpha\beta} / \partial Q_{\gamma_p}$, $D_{\alpha}^{\gamma} \equiv \partial D_{\alpha} / \partial Q_{\gamma_p}$, and the index p is left implicit. The Hamiltonian is invariant under mirror reflections with respect to each coordinate axis. Taking account of the symmetry of the displacement coordinate and the fact that m_x interchanges indices of the exchange tensor, we have that

$$\begin{aligned} \sigma_x \mathbf{J}^{\gamma} \sigma_x &= (1 - 2\delta_{x,\gamma}) \tilde{\mathbf{J}}^{\gamma} \\ \sigma_y \mathbf{J}^{\gamma} \sigma_y &= (1 - 2\delta_{y,\gamma}) \mathbf{J}^{\gamma} \\ \sigma_z \mathbf{J}^{\gamma} \sigma_z &= (1 - 2\delta_{z,\gamma}) \mathbf{J}^{\gamma}. \end{aligned} \quad (62)$$

As a result of this symmetry we have that $\mathbf{J}^x = 0$,

$$\begin{aligned} \mathbf{J}^y &= \begin{bmatrix} 0 & D_z^y & 0 \\ -D_z^y & 0 & 0 \\ 0 & 0 & 0 \end{bmatrix}, \\ \mathbf{J}^z &= \begin{bmatrix} 0 & 0 & -D_y^z \\ 0 & 0 & 0 \\ D_y^z & 0 & 0 \end{bmatrix}. \end{aligned} \quad (63)$$

We construct the trilinear spin-phonon interaction, V , as

$$V = \sum_p (Q_{y_p} D_z^{y_p} C_y + Q_{z_p} D_y^{z_p} C_z), \quad (64)$$

where

$$C_{\alpha} = \sum_n [S_x(n) S_{\alpha}(n+1) - S_{\alpha}(n) S_x(n+1)]. \quad (65)$$

Now we replace the spins by their equilibrium values. We note that each spin component belongs to a separate representation and we write

$$\begin{aligned} S_x(n) &= S_x(q) e^{inqa} + S_x(q)^* e^{-inqa}, \\ S_y(n) &= S_y(q) e^{inqa} + S_y(q)^* e^{-inqa}, \\ S_z(n) &= S_z(q) e^{inqa} + S_z(q)^* e^{-inqa}. \end{aligned} \quad (66)$$

Then, keeping only those terms which survive the sum over n we have

$$\begin{aligned} V &= 4N \sin(qa) \sum_p [Q_{y_p} D_z^{y_p} r_x(q) r_y(q) \sin(\phi_x - \phi_y) \\ &\quad + Q_{z_p} D_y^{z_p} r_z(q) r_x(q) \sin(\phi_x - \phi_z)], \end{aligned} \quad (67)$$

TABLE VI: Basis spin functions for sites #1 and #2 in the unit cell in terms of the complex-valued Fourier components $S_\alpha(q)$ for irreps characterized by the eigenvalues of m_y and the glide operation m_z .

Γ	m_y	m_z	$\mathbf{S}(\#1)$	$\mathbf{S}(\#2)$
Γ_1	+	+	$(S_x(q), 0, S_z(q))$	$(S_x(q), 0, -S_z(q))$
Γ_2	+	-	$(S_x(q), 0, S_z(q))$	$(-S_x(q), 0, -S_z(q))$
Γ_3	-	+	$(0, S_y(q), 0)$	$(0, S_y(q), 0)$
Γ_4	-	-	$(0, S_y(q), 0)$	$(0, -S_y(q), 0)$

where N is the total number of Ni spins and we set $S_\alpha(q) = r_\alpha(q)e^{i\phi_\alpha}$, where $r_\alpha(q)$ is real. As found before^{3,4,7} this interaction is only nonzero when a) two different representations are condensed and b) the two representation have different phases ϕ . In view of our previous results, it is clear that the appearance of only strain derivatives of the DM vector is an artifact of the rather high symmetry of this coplanar model.

B. Unit cell with four atoms

Now we consider the noncoplanar toy model shown in the right panel of Fig. 8. The first two symmetry relations of Eq. (62) remain valid, but the third one now results from the glide plane which involves a translation along the chain. If \mathbf{J}_\pm^α denotes the strain derivative of the exchange tensor for coupling sites $2n$ and $2n+1$, and \mathbf{J}_\pm^α that for sites $2n+1$ and $2n+2$, then we have

$$\mathbf{J}_\pm^x = \begin{bmatrix} 0 & 0 & \pm J_{xz}^x \\ 0 & 0 & 0 \\ \pm J_{xz}^x & 0 & 0 \end{bmatrix}, \quad (68)$$

$$\mathbf{J}_\pm^y = \begin{bmatrix} 0 & D_z^y & 0 \\ -D_z^y & 0 & \pm J_{yz}^y \\ 0 & \pm J_{yz}^y & 0 \end{bmatrix}, \quad (69)$$

$$\mathbf{J}_\pm^z = \begin{bmatrix} \pm J_{xx}^z & 0 & -D_y^z \\ 0 & \pm J_{yy}^z & 0 \\ D_y^z & 0 & \pm J_{zz}^z \end{bmatrix}. \quad (70)$$

Next we characterize the spin structure. There are four irreps for which the basis functions are listed in Table VI. Thus we write for spins #1 (\mathbf{S}_1) and #2 (\mathbf{S}_2) in the unit cell,

$$S_{1,x}(X) = [S_x^{(1)}(q) + S_x^{(2)}(q)]e^{iqX} + [S_x^{(1)}(q)^* + S_x^{(2)}(q)^*]e^{-iqX}, \quad (71)$$

$$S_{1,y}(X) = [S_y^{(3)}(q) + S_y^{(4)}(q)]e^{iqX} + [S_y^{(3)}(q)^* + S_y^{(4)}(q)^*]e^{-iqX}, \quad (72)$$

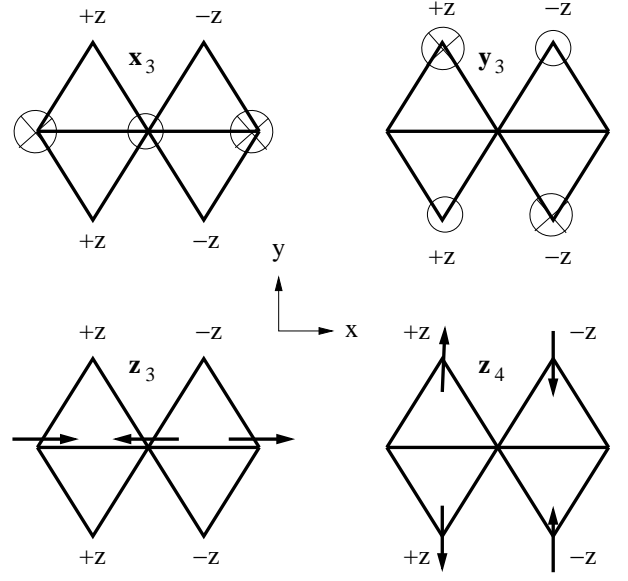


FIG. 9: Generalized displacements which transform like vectors. Open circles (circles with inscribed "x") are displacements out of (into) the page. The sites at positive or negative z are indicated. The upper panels show modes in which the atoms move only in the z -direction. Upper left: an x -like mode x_3 . Upper right: a y -like mode y_3 . The lower panels show z -like modes. Left: z_3 with motion only along the x -axis and right: z_4 with motion only along the y -axis.

$$S_{1,z}(X) = [S_z^{(1)}(q) + S_z^{(2)}(q)]e^{iqX} + [S_z^{(1)}(q)^* + S_z^{(2)}(q)^*]e^{-iqX}, \quad (73)$$

$$S_{2,x}(X) = [S_x^{(1)}(q) - S_x^{(2)}(q)]e^{iqX} + [S_x^{(1)}(q)^* - S_x^{(2)}(q)^*]e^{-iqX}, \quad (74)$$

$$S_{2,y}(X) = [S_y^{(3)}(q) - S_y^{(4)}(q)]e^{iqX} + [S_y^{(3)}(q)^* - S_y^{(4)}(q)^*]e^{-iqX}, \quad (75)$$

$$S_{2,z}(X) = [-S_z^{(1)}(q) + S_z^{(2)}(q)]e^{iqX} + [-S_z^{(1)}(q)^* + S_z^{(2)}(q)^*]e^{-iqX}, \quad (76)$$

where the superscript labels the irrep as in Table VI. Thereby we find the trilinear spin-phonon coupling (when the spin operators are replaced by their values:

$$V = 4N \sin(qa) \sum_p \left[U Q_{x_p} J_{xz}^{x_p} + Q_{y_p} (V J_{yz}^{y_p} + W D_z^{y_p}) + Q_{z_p} \left(X D_y^{z_p} + \sum_{\alpha=x,y,z} Y_\alpha J_{\alpha\alpha}^{z_p} \right) \right], \quad (77)$$

where

$$U = \Im \left(S_x^{(1)}(q)^* S_z^{(1)}(q) + S_x^{(2)}(q) S_z^{(2)}(q)^* \right) \quad (78)$$

$$V = \Im \left(S_y^{(4)}(q) S_z^{(2)}(q)^* + S_z^{(1)}(q) S_y^{(3)}(q)^* \right) \quad (79)$$

$$W = \Im \left(S_x^{(1)}(q) S_y^{(3)}(q)^* + S_x^{(2)}(q)^* S_y^{(4)}(q) \right) \quad (80)$$

$$X = \Im \left(S_x^{(1)}(q)^* S_z^{(2)}(q) + S_x^{(2)}(q) S_z^{(1)}(q)^* \right) \quad (81)$$

$$Y_x = \Im \left(S_x^{(1)}(q)^* S_x^{(2)}(q) \right) \quad (82)$$

$$Y_y = \Im \left(S_y^{(3)}(q)^* S_y^{(4)}(q) \right) \quad (83)$$

$$Y_z = \Im \left(S_z^{(1)}(q) S_z^{(2)}(q)^* \right) \quad (84)$$

The general symmetry arguments indicate that there can not be a polarization along \hat{i} . We see that U vanishes because all the components within a single representation have the same phase, so that, for instance, $S_x^{(1)}(q) S_z^{(1)}(q)^*$ is real. Here we see that, depending on the spin structure the spontaneous polarization can either be along \hat{j} (if either both irreps #1 and #3 are active or both irreps #2 and #4 are active) or along \hat{k} (if either both irreps #1 and #2 are active or both irreps #3 and #4 are active.) These results are exactly what the phenomenological analysis would give.

VIII. CONCLUSIONS

In this paper we present neutron scattering measurements of phonons in NVO, the first-principles computation of the zone-center phonons and their symmetry analysis. We identified two particularly interesting phonons among the twelve B_{2u} modes which have the right symmetry to induce the experimentally observed dipole moment along the \mathbf{b} -axis in NVO. Using the calculated atomic charges and the eigenvectors we conclude that the required distortion to induce the observed dipole moment is small (0.001 Å) and would be difficult to observe directly by neutron powder diffraction. Finally, we present a symmetry analysis to characterize the microscopic magnetoelectric coupling in $\text{Ni}_3\text{V}_2\text{O}_8$. The method can easily be applied to similar systems such as TbMnO_3 . The result of this analysis is that we can specify those strain derivatives of the exchange tensor which should now be the targets of more fundamental quantum calculations, perhaps based on the LDA¹¹ or similar schemes. (These results are given in Eqs. (52)-(55), where the superscript indicates the component of the gradient.) In Subsec. VIB we show how these gradients lead to an evaluation of the spontaneous polarization from first principles. In Sec. VII we also studied some structurally simpler toy models. A general conclusion is that the local site symmetry in NVO is low enough that almost all strain derivatives of the exchange tensor are involved. It is true that the Dzyaloshinskii-Moriya interaction must be present (and, of course, it is allowed in such low symmetry systems). In the presence of such interactions ferroelectricity results from the strain dependence of all the components of the exchange tensor, even that of the isotropic exchange interaction.

Acknowledgments

This work was supported in part by the Israel US Binational Science Foundation under grant number 2000073. We thank C. Broholm for providing us the NVO powder samples used in this study.

APPENDIX A: NEXT-NEAREST NEIGHBOR SPINE INTERACTIONS

In this section we consider next-nearest neighbor (nnn) interactions between spins on a given spine. Since only the gradients with respect to Q_{y_p} are needed, we only consider those here. We set

$$\frac{\partial J_{\alpha\beta}(1, 1')}{\partial Q_{y_p}} = V_{\alpha\beta}^{y_p}. \quad (A1)$$

The operation 2_y takes this bond into itself with reversed indices. So, taking account of the transformation properties of Q_{y_p} , we require that

$$2_y \mathbf{V}^{y_p} = \tilde{\mathbf{V}}^{y_p}, \quad (A2)$$

where 2_y is the two-fold rotation operator. In terms of matrices, this relation is

$$2_y \mathbf{V}^{y_p} 2_y = \tilde{\mathbf{V}}^{y_p}, \quad (A3)$$

where $2_y = \sigma_x \sigma_z$. Thus

$$\mathbf{V}^{y_p} = \begin{bmatrix} K_{xx}^y & E_z^y & K_{xz}^y \\ -E_z^y & K_{yy}^y & E_x^y \\ K_{xz}^y & -E_x^y & K_{zz}^y \end{bmatrix}. \quad (A4)$$

We have that

$$\frac{\partial J_{\alpha\beta}(2, 2')}{\partial Q_{y_p}} = -2_x \mathbf{V}^{y_p} 2_x, \quad (A5)$$

so that

$$\frac{\partial J_{\alpha\beta}(2, 2')}{\partial Q_{y_p}} = \begin{bmatrix} -K_{xx}^y & E_z^y & K_{xz}^y \\ -E_z^y & -K_{yy}^y & -E_x^y \\ K_{xz}^y & E_x^y & -K_{zz}^y \end{bmatrix}. \quad (A6)$$

We have that

$$\frac{\partial J_{\alpha\beta}(3', 3)}{\partial Q_{y_p}} = -\sigma_y \mathbf{V}^{\gamma_p} \sigma_y, \quad (A7)$$

so that

$$\frac{\partial J_{\alpha\beta}(3', 3)}{\partial Q_{y_p}} = \begin{bmatrix} -K_{xx}^y & E_z^y & -K_{xz}^y \\ -E_z^y & -K_{yy}^y & E_x^y \\ -K_{xz}^y & -E_x^y & -K_{zz}^y \end{bmatrix}. \quad (A8)$$

We have that

$$\frac{\partial J_{\alpha\beta}(4', 4)}{\partial Q_{y_p}} = \sigma_x \tilde{\mathbf{V}}^{\gamma_p} \sigma_x, \quad (A9)$$

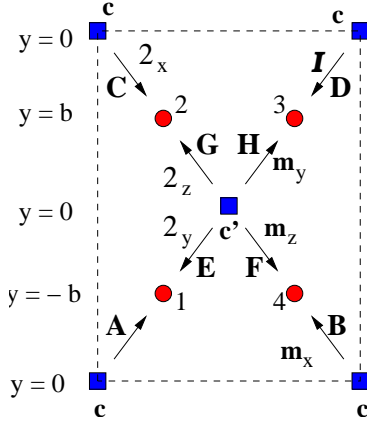


FIG. 10: As Fig. 7. Here we show the eight different nearest-neighbor spine-cross tie interactions, which we label A ... H. The arrow points from the first site index to the second site index. We also give the symmetry operation one has to apply to interaction A to get each of the other interactions.

so that

$$\frac{\partial J_{\alpha\beta}(4', 4)}{\partial Q_{y_p}} = \begin{bmatrix} K_{xx}^y & E_z^y & -K_{xz}^y \\ -E_x^y & K_{yy}^y & -E_x^y \\ -K_{xz}^y & E_x^y & K_{zz}^y \end{bmatrix}. \quad (\text{A10})$$

APPENDIX B: SPINE CROSS-TIE INTERACTIONS

In this section we analyze the spine-cross tie interactions, in Fig. 10, again keeping only derivative with respect to Q_{y_p} . We set the interaction of type A to be

$$\frac{\partial J_{\alpha\beta}(c, 1)}{\partial Q_{y_p}} = W_{\alpha\beta}^{y_p}, \quad (\text{B1})$$

so that (when the index p is suppressed)

$$\mathbf{W}^y = \begin{bmatrix} L_{xx}^y & L_{xy}^y + F_z^y & L_{xz}^y - F_y^y \\ L_{xy}^y - F_z^y & L_{yy}^y & L_{yz}^y + F_x^y \\ L_{xz}^y + F_y^y & L_{yz}^y - F_x^y & L_{zz}^y \end{bmatrix}. \quad (\text{B2})$$

We have that

$$\frac{\partial \mathbf{J}(c, 4)}{\partial Q_{y_p}} = \boldsymbol{\sigma}_x \mathbf{W}^{\gamma_p} \boldsymbol{\sigma}_x, \quad (\text{B3})$$

so that

$$\frac{\partial \mathbf{J}(c, 4)}{\partial Q_{y_p}} = \begin{bmatrix} L_{xx}^y & -L_{xy}^y - F_z^y & -L_{xz}^y + F_y^y \\ -L_{xy}^y + F_z^y & L_{yy}^y & L_{yz}^y + F_x^y \\ -L_{xz}^y - F_y^y & L_{yz}^y - F_x^y & L_{zz}^y \end{bmatrix}. \quad (\text{B4})$$

We have that

$$\frac{\partial \mathbf{J}(c, 2)}{\partial Q_{y_p}} = -2_x \mathbf{W}^{y_p} 2_x, \quad (\text{B5})$$

so that

$$\frac{\partial \mathbf{J}(c, 2)}{\partial Q_{y_p}} = \begin{bmatrix} -L_{xx}^y & L_{xy}^y + F_z^y & L_{xz}^y - F_y^y \\ L_{xy}^y - F_z^y & -L_{yy}^y & -L_{yz}^y - F_x^y \\ L_{xz}^y + F_y^y & -L_{yz}^y + F_x^y & -L_{zz}^y \end{bmatrix}. \quad (\text{B6})$$

We have that

$$\frac{\partial \mathbf{J}(c, 3)}{\partial Q_{y_p}} = -\mathcal{I} \mathbf{W}^{\gamma_p} \mathcal{I}, \quad (\text{B7})$$

so that

$$\frac{\partial \mathbf{J}(c, 3)}{\partial Q_{y_p}} = \begin{bmatrix} -L_{xx}^y & -L_{xy}^y - F_z^y & -L_{xz}^y + F_y^y \\ -L_{xy}^y + F_z^y & -L_{yy}^y & -L_{yz}^y - F_x^y \\ -L_{xz}^y - F_y^y & -L_{yz}^y + F_x^y & -L_{zz}^y \end{bmatrix}. \quad (\text{B8})$$

We have that

$$\frac{\partial \mathbf{J}(c', 1)}{\partial Q_{y_p}} = 2_y \mathbf{W} 2_y, \quad (\text{B9})$$

so that

$$\frac{\partial \mathbf{J}(c', 1)}{\partial Q_{y_p}} = \begin{bmatrix} L_{xx}^y & -L_{xy}^y - F_z^y & L_{xz}^y - F_y^y \\ -L_{xy}^y + F_z^y & L_{yy}^y & -L_{yz}^y - F_x^y \\ L_{xz}^y + F_y^y & -L_{yz}^y + F_x^y & L_{zz}^y \end{bmatrix}. \quad (\text{B10})$$

We have that

$$\frac{\partial \mathbf{J}(c', 4)}{\partial Q_{y_p}} = \boldsymbol{\sigma}_z \mathbf{W}^{\gamma_p} \boldsymbol{\sigma}_z, \quad (\text{B11})$$

so that

$$\frac{\partial \mathbf{J}(c', 4)}{\partial Q_{y_p}} = \begin{bmatrix} L_{xx}^y & L_{xy}^y + F_z^y & -L_{xz}^y + F_y^y \\ L_{xy}^y - F_z^y & L_{yy}^y & -L_{yz}^y - F_x^y \\ -L_{xz}^y - F_y^y & -L_{yz}^y + F_x^y & L_{zz}^y \end{bmatrix}. \quad (\text{B12})$$

We have that

$$\frac{\partial \mathbf{J}(c', 2)}{\partial Q_{y_p}} = -2_z \mathbf{W}^{\gamma_p} 2_z, \quad (\text{B13})$$

so that

$$\frac{\partial \mathbf{J}(c', 2)}{\partial Q_{y_p}} = \begin{bmatrix} -L_{xx}^y & -L_{xy}^y - F_z^y & L_{xz}^y - F_y^y \\ -L_{xy}^y + F_z^y & -L_{yy}^y & L_{yz}^y + F_x^y \\ L_{xz}^y + F_y^y & L_{yz}^y - F_x^y & -L_{zz}^y \end{bmatrix}. \quad (\text{B14})$$

We have that

$$\frac{\partial \mathbf{J}(c', 3)}{\partial Q_{y_p}} = -\boldsymbol{\sigma}_y \mathbf{W}^{\gamma_p} \boldsymbol{\sigma}_y, \quad (\text{B15})$$

so that

$$\frac{\partial \mathbf{J}(c', 3)}{\partial Q_{y_p}} = \begin{bmatrix} -L_{xx}^y & L_{xy}^y + F_z^y & -L_{xz}^y + F_y^y \\ L_{xy}^y - F_z^y & -L_{yy}^y & L_{yz}^y + F_x^y \\ -L_{xz}^y - F_y^y & L_{yz}^y - F_x^y & -L_{zz}^y \end{bmatrix}. \quad (\text{B16})$$

APPENDIX C: SPIN-PHONON INTERACTION

1. nn spine interactions

Now we collect terms involving J_{xx}^y :

$$\begin{aligned}
V_y(J_{xx}^y) &= Q_y J_{xx}^y \sum_{uc} \left[S_x(1)S_x(4) - S_x(2)S_x(3) \right. \\
&\quad \left. + S_x(4)S_x(1') - S_x(3)S_x(2') \right] \\
&= Q_y J_{xx}^y \sum_{uc} e^{iqx14} \left[(a_x + ib_x)(-a_x^* + ib_x^*) \right. \\
&\quad \left. - (-a_x + ib_x)(a_x^* + ib_x^*) \right. \\
&\quad \left. + (-a_x - ib_x)(a_x^* - ib_x^*) \right. \\
&\quad \left. - (a_x - ib_x)(-a_x^* - ib_x^*) \right] + \text{c. c.} \\
&= 4Q_y J_{xx}^y N_{uc} (e^{iqx14} [ia_x b_x^* - ib_x a_x^*] + \text{c. c.}) \\
&= -16N_{uc} Q_y J_{xx}^y \cos(qa/2) \Im[a_x b_x^*]. \quad (\text{C1})
\end{aligned}$$

Now we collect terms involving J_{yy}^y :

$$\begin{aligned}
V_y(J_{yy}^y) &= Q_y J_{yy}^y \sum_{uc} \left[S_y(1)S_y(4) - S_y(2)S_y(3) \right. \\
&\quad \left. + S_y(4)S_y(1') - S_y(3)S_y(2') \right] \\
&= Q_y J_{yy}^y \sum_{uc} e^{iqx14} \left[(ia_y + b_y)(ia_y^* - b_y^*) \right. \\
&\quad \left. - (ia_y - b_y)(ia_y^* + b_y^*) \right. \\
&\quad \left. + (-ia_y - b_y)(-ia_y^* + b_y^*) \right. \\
&\quad \left. - (-ia_y + b_y)(-ia_y^* - b_y^*) \right] + \text{c. c.} \\
&= 4Q_y J_{yy}^y N_{uc} (e^{iqx14} [-ia_y b_y^* + ib_y a_y^*] + \text{c. c.}) \\
&= 16N_{uc} Q_y J_{yy}^y \cos(qa/2) \Im[a_y b_y^*]. \quad (\text{C2})
\end{aligned}$$

Now we collect terms involving J_{zz}^y :

$$\begin{aligned}
V_y(J_{zz}^y) &= Q_y J_{zz}^y \sum_{uc} \left[S_z(1)S_z(4) - S_z(2)S_z(3) \right. \\
&\quad \left. + S_z(4)S_z(1') - S_z(3)S_z(2') \right] \\
&= Q_y J_{zz}^y \sum_{uc} e^{iqx14} \left[(a_z + ib_z)(a_z^* - ib_z^*) \right. \\
&\quad \left. - (a_z - ib_z)(a_z^* + ib_z^*) \right. \\
&\quad \left. + (a_z + ib_z)(a_z^* - ib_z^*) \right. \\
&\quad \left. - (a_z - ib_z)(a_z^* + ib_z^*) \right] + \text{c. c.} \\
&= 4Q_y J_{zz}^y N_{uc} (e^{iqx14} [-ia_z b_z^* + ib_z a_z^*] + \text{c. c.}) \\
&= 16N_{uc} Q_y J_{zz}^y \cos(qa/2) \Im[a_z b_z^*]. \quad (\text{C3})
\end{aligned}$$

Now we collect terms involving J_{yz}^y :

$$\begin{aligned}
V_y(J_{yz}^y) &= Q_y J_{yz}^y \sum_{uc} \left[S_y(1)S_z(4) + S_z(1)S_y(4) \right. \\
&\quad \left. - S_z(2)S_y(3) - S_y(2)S_z(3) \right. \\
&\quad \left. - S_y(4)S_z(1') - S_z(4)S_y(1') \right. \\
&\quad \left. + S_y(3)S_z(2') + S_z(3)S_y(2') \right] \\
&= Q_y J_{yz}^y \sum_{uc} e^{iqx14} \left[(ia_y + b_y)(a_z^* - ib_z^*) \right. \\
&\quad \left. + (a_z + ib_z)(ia_y^* - b_y^*) \right. \\
&\quad \left. - (a_z - ib_z)(ia_y^* + b_y^*) \right. \\
&\quad \left. - (ia_y - b_y)(a_z^* + ib_z^*) \right. \\
&\quad \left. - (-ia_y - b_y)(a_z^* - ib_z^*) \right. \\
&\quad \left. - (a_z + ib_z)(-ia_y^* + b_y^*) \right. \\
&\quad \left. + (-ia_y + b_y)(a_z^* + ib_z^*) \right. \\
&\quad \left. + (a_z - ib_z)(-ia_y^* - b_y^*) \right] + \text{c. c.} \\
&= 4Q_y J_{yz}^y N_{uc} (e^{iqx14} [a_y b_z^* + b_y a_z^* - a_z b_y^* - b_z a_y^*] \\
&\quad + \text{c. c.}) \\
&= -16N_{uc} Q_y \sin(qa/2) J_{yz}^y \Im[a_y^* b_z + b_y^* a_z]. \quad (\text{C4})
\end{aligned}$$

Now we collect terms proportional to D_z^y :

$$\begin{aligned}
V_y(D_z^y) &= Q_y D_z^y \sum_{uc} \left[S_x(1)S_y(4) - S_y(1)S_x(4) \right. \\
&\quad \left. + S_x(2)S_y(3) - S_y(2)S_x(3) \right. \\
&\quad \left. + S_x(4)S_y(1') - S_y(4)S_x(1') \right. \\
&\quad \left. + S_x(3)S_y(2') - S_y(3)S_x(2') \right] \\
&= Q_y D_z^y \sum_{uc} e^{iqx14} \left[(a_x + ib_x)(ia_y^* - b_y^*) \right. \\
&\quad \left. - (ia_y + b_y)(-a_x^* + ib_x^*) \right. \\
&\quad \left. + (-a_x + ib_x)(ia_y^* + b_y^*) \right. \\
&\quad \left. - (ia_y - b_y)(a_x^* + ib_x^*) \right. \\
&\quad \left. + (-a_x - ib_x)(-ia_y^* + b_y^*) \right. \\
&\quad \left. - (-ia_y - b_y)(a_x^* - ib_x^*) \right. \\
&\quad \left. + (a_x - ib_x)(-ia_y^* - b_y^*) \right. \\
&\quad \left. - (-ia_y + b_y)(-a_x^* - ib_x^*) \right] + \text{c. c.} \\
&= 4Q_y D_z^y N_{uc} (e^{iqx14} [-a_x b_y^* - b_x a_y^* + a_y b_x^* + b_y a_x^*] \\
&\quad + \text{c. c.}) \\
&= -16N_{uc} Q_y \sin(qa/2) D_z^y \Im[a_y^* b_x + b_y^* a_x]. \quad (\text{C5})
\end{aligned}$$

Now we collect terms proportional to D_y^y :

$$\begin{aligned}
V_y(D_y^y) &= Q_y D_y^y \sum_{uc} \left[-S_x(1)S_z(4) + S_z(1)S_x(4) \right. \\
&\quad \left. - S_x(2)S_z(3) + S_z(2)S_x(3) \right]
\end{aligned}$$

$$\begin{aligned}
& +S_x(4)S_z(1') - S_z(4)S_x(1') \\
& +S_x(3)S_z(2') - S_z(3)S_x(2') \Big] \\
= & Q_y D_y^y \sum_{uc} e^{iqx14} \left[-(a_x + ib_x)(a_z^* - ib_z^*) \right. \\
& + (a_z + ib_z)(-a_x^* + ib_x^*) \\
& - (-a_x + ib_x)(a_z^* + ib_z^*) \\
& + (a_z - ib_z)(a_x^* + ib_x^*) \\
& + (-a_x - ib_x)(a_z^* - ib_z^*) \\
& - (a_z + ib_z)(a_x^* - ib_x^*) \\
& \left. + (a_x - ib_x)(a_z^* + ib_z^*) \right] \\
& - (a_z - ib_z)(-a_x^* - ib_x^*) \Big] \\
& + \text{c. c.} \\
= & 4Q_y D_y^y N_{uc} \left(e^{iqx14} i [a_x b_z^* - b_x a_z^* + a_z b_x^* - b_z a_x^*] \right. \\
& \left. + \text{c. c.} \right) \\
= & -16N_{uc} Q_y \cos(qa/2) D_y^y \Im [a_x b_z^* + b_x^* a_z] . \quad (\text{C6})
\end{aligned}$$

2. nnn spine interactions

First we consider terms proportional to K_{xx}^y (where we omit the p index):

$$\begin{aligned}
V_y(K_{xx}^y) &= Q_y K_{xx}^y \sum_{uc} [S_x(1)S_x(1') - S_x(2)S_x(2') \\
&\quad - S_x(3)S_x(3') + S_x(4)S_x(4')] \\
&= N_{uc} Q_y K_{xx}^y [t_{xx} + t_{xx}^*] , \quad (\text{C7})
\end{aligned}$$

where

$$\begin{aligned}
t_{xx} &= e^{-iqa} [(a_{s,x} + ib_{s,x})(a_{s,x}^* - ib_{s,x}^*) \\
&\quad - (-a_{s,x} + ib_{s,x})(-a_{s,x}^* - ib_{s,x}^*) \\
&\quad - (a_{s,x} - ib_{s,x})(a_{s,x}^* + ib_{s,x}^*) \\
&\quad + (-a_{s,x} - ib_{s,x})(-a_{s,x}^* + ib_{s,x}^*)] \\
&= e^{-iqa} [-4ia_{s,x}b_{s,x}^* + 4ia_{s,x}^*b_{s,x}] \\
&= 8e^{-iqa} \Im [a_{s,x}b_{s,x}^*] , \quad (\text{C8})
\end{aligned}$$

so that

$$V_y(K_{xx}^y) = 16N_{uc} Q_y K_{xx}^y \cos(qa) \Im [a_{s,x}b_{s,x}^*] . \quad (\text{C9})$$

Next, we consider terms proportional to K_{yy}^y :

$$\begin{aligned}
V_y(K_{yy}^y) &= Q_y K_{yy}^y \sum_{uc} [S_y(1)S_y(1') - S_y(2)S_y(2') \\
&\quad - S_y(3)S_y(3') + S_y(4)S_y(4')] \\
&= N_{uc} Q_y K_{yy}^y [t_{yy} + t_{yy}^*] , \quad (\text{C10})
\end{aligned}$$

where

$$\begin{aligned}
t_{yy} &= e^{-iqa} [(ia_{s,y} + b_{s,y})(-ia_{s,y}^* + b_{s,y}^*) \\
&\quad - (ia_{s,y} - b_{s,y})(-ia_{s,y}^* - b_{s,y}^*)]
\end{aligned}$$

$$\begin{aligned}
& - (-ia_{s,y} + b_{s,y})(ia_{s,y}^* + b_{s,y}^*) \\
& + (-ia_{s,y} - b_{s,y})(ia_{s,y}^* - b_{s,y}^*)] \\
&= e^{-iqa} [4ia_{s,y}b_{s,y}^* - 4ia_{s,y}^*b_{s,y}] \\
&= 8e^{-iqa} \Im [a_{s,y}^*b_{s,y}] , \quad (\text{C11})
\end{aligned}$$

so that

$$V_y(K_{yy}^y) = 16N_{uc} Q_y K_{yy}^y \cos(qa) \Im [a_{s,y}^*b_{s,y}] . \quad (\text{C12})$$

Next, we consider terms proportional to K_{zz}^y :

$$\begin{aligned}
V_y(K_{zz}^y) &= Q_y K_{zz}^y \sum_{uc} (S_z(1)S_z(1') - S_z(2)S_z(2') \\
&\quad - S_z(3)S_z(3') + S_z(4)S_z(4')) \\
&= N_{uc} Q_y K_{zz}^y [t_{zz} + t_{zz}^*] , \quad (\text{C13})
\end{aligned}$$

where

$$\begin{aligned}
t_{zz} &= e^{-iqa} [(a_{s,z} + ib_{s,z})(a_{s,z}^* - ib_{s,z}^*) \\
&\quad - (a_{s,z} - ib_{s,z})(a_{s,z}^* + ib_{s,z}^*) \\
&\quad - (a_{s,z} - ib_{s,z})(a_{s,z}^* + ib_{s,z}^*) \\
&\quad + (a_{s,z} + ib_{s,z})(a_{s,z}^* - ib_{s,z}^*)] \\
&= e^{-iqa} [-4ia_{s,z}b_{s,z}^* + 4ia_{s,z}^*b_{s,z}] \\
&= 8e^{-iqa} \Im [a_{s,z}b_{s,z}^*] , \quad (\text{C14})
\end{aligned}$$

so that

$$V_y(K_{zz}^y) = 16N_{uc} Q_y K_{zz}^y \cos(qa) \Im [a_{s,z}b_{s,z}^*] . \quad (\text{C15})$$

Now we consider terms proportional to E_z^y :

$$\begin{aligned}
V_y(E_z^y) &= Q_y E_z^y \sum_{uc} [S_x(1)S_y(1') - S_y(1)S_x(1') \\
&\quad + S_x(2)S_y(2') - S_y(2)S_x(2') \\
&\quad + S_x(3')S_y(3) - S_y(3')S_x(3) \\
&\quad + S_x(4')S_y(4) - S_y(4')S_x(4)] \\
&= N_{uc} Q_y E_z^y [t_{zy} + t_{zy}^*] , \quad (\text{C16})
\end{aligned}$$

where

$$\begin{aligned}
t_{zy} &= e^{-iqa} [(a_{s,x} + ib_{s,x})(-ia_{s,y}^* + b_{s,y}^*) \\
&\quad - (ia_{s,y} + b_{s,y})(a_{s,x}^* - ib_{s,x}^*) \\
&\quad + (-a_{s,x} + ib_{s,x})(-ia_{s,y}^* - b_{s,y}^*) \\
&\quad - (ia_{s,y} - b_{s,y})(-a_{s,x}^* - ib_{s,x}^*) \\
&\quad + (a_{s,x} - ib_{s,x})(ia_{s,y}^* + b_{s,y}^*) \\
&\quad - (-ia_{s,y} + b_{s,y})(a_{s,x}^* + ib_{s,x}^*) \\
&\quad + (-a_{s,x} - ib_{s,x})(ia_{s,y}^* - b_{s,y}^*) \\
&\quad - (-ia_{s,y} - b_{s,y})(-a_{s,x}^* + ib_{s,x}^*)] \\
&= 4e^{-iqa} [a_{s,x}b_{s,y}^* + b_{s,x}a_{s,y}^* - a_{s,y}b_{s,x}^* - b_{s,y}a_{s,x}^*] \\
&= 8ie^{-iqa} \Im [a_{s,x}b_{s,y}^* + b_{s,x}a_{s,y}^*] , \quad (\text{C17})
\end{aligned}$$

so that

$$V_y(E_z^y) = 16N_{uc} Q_y E_z^y \sin(qa) \Im [a_{s,x}b_{s,y}^* + b_{s,x}a_{s,y}^*] . \quad (\text{C18})$$

Now we consider terms proportional to E_x^y :

$$\begin{aligned}
V_y(E_x^y) &= Q_y E_x^y \sum_{uc} [S_y(1)S_z(1') - S_z(1)S_y(1') \\
&\quad - S_y(2)S_z(2') + S_z(2)S_y(2') \\
&\quad + S_y(3)S_z(3) - S_z(3)S_y(3) \\
&\quad - S_y(4)S_z(4) + S_z(4)S_y(4)] \\
&= N_{uc} Q_y E_x^y [t_{xy} + t_{xy}^*], \tag{C19}
\end{aligned}$$

where

$$\begin{aligned}
t_{xy} &= e^{-iqa} [(ia_{s,y} + b_{s,y})(a_{s,z}^* - ib_{s,z}^*) \\
&\quad - (a_{s,z} + ib_{s,z})(-ia_{s,y}^* + b_{s,y}^*) \\
&\quad - (ia_{s,y} - b_{s,y})(a_{s,z}^* + ib_{s,z}^*) \\
&\quad + (a_{s,z} - ib_{s,z})(-ia_{s,y}^* - b_{s,y}^*) \\
&\quad + (-ia_{s,y} + b_{s,y})(a_{s,z}^* + ib_{s,z}^*) \\
&\quad - (a_{s,z} - ib_{s,z})(ia_{s,y}^* + b_{s,y}^*) \\
&\quad - (-ia_{s,y} - b_{s,y})(a_{s,z}^* - ib_{s,z}^*) \\
&\quad + (a_{s,z} + ib_{s,z})(ia_{s,y}^* - b_{s,y}^*)] \\
&= 4e^{-iqa} [a_{s,y}b_{s,z}^* + b_{s,y}a_{s,z}^* \\
&\quad - a_{s,z}b_{s,y}^* - b_{s,z}a_{s,y}^*] \\
&= 8ie^{-iqa} \Im[a_{s,y}b_{s,z}^* + b_{s,y}a_{s,z}^*], \tag{C20}
\end{aligned}$$

so that

$$V_y(E_x^y) = 16N_{uc}Q_y E_x^y \sin(qa) \Im[a_{s,y}b_{s,z}^* + b_{s,y}a_{s,z}^*] \tag{C21}$$

Now we consider terms proportional to K_{xz}^y :

$$\begin{aligned}
V_y(K_{xz}^y) &= Q_y K_{xz}^y \sum_{uc} [S_x(1)S_z(1') + S_z(1)S_x(1') \\
&\quad + S_x(2)S_z(2') + S_z(2)S_x(2') \\
&\quad - S_x(3)S_z(3') - S_z(3)S_x(3') \\
&\quad - S_x(4)S_z(4') - S_z(4)S_x(4')] \\
&= N_{uc} Q_y K_{xz}^y [t_{xz} + t_{xz}^*], \tag{C22}
\end{aligned}$$

where

$$\begin{aligned}
t_{xz} &= e^{-iqa} [(a_{s,x} + ib_{s,x})(a_{s,z}^* - ib_{s,z}^*) \\
&\quad + (a_{s,z} + ib_{s,z})(a_{s,x}^* - ib_{s,x}^*) \\
&\quad + (-a_{s,x} + ib_{s,x})(a_{s,z}^* + ib_{s,z}^*) \\
&\quad + (a_{s,z} - ib_{s,z})(-a_{s,x}^* - ib_{s,x}^*) \\
&\quad - (a_{s,x} - ib_{s,x})(a_{s,z}^* + ib_{s,z}^*) \\
&\quad - (a_{s,z} - ib_{s,z})(a_{s,x}^* + ib_{s,x}^*) \\
&\quad - (-a_{s,x} - ib_{s,x})(a_{s,z}^* - ib_{s,z}^*) \\
&\quad - (a_{s,z} + ib_{s,z})(-a_{s,x}^* + ib_{s,x}^*)] \\
&= 4ie^{-iqa} [-a_{s,x}b_{s,z}^* + b_{s,x}a_{s,z}^* - a_{s,z}b_{s,x}^* + b_{s,z}a_{s,x}^*] \\
&= 8e^{-iqa} \Im[a_{s,x}b_{s,z}^* + a_{s,z}b_{s,x}^*], \tag{C23}
\end{aligned}$$

so that

$$\begin{aligned}
V_y(K_{xz}^y) &= 16N_{uc}Q_y K_{xz}^y \cos(qa) \\
&\quad \times \Im[a_{s,x}b_{s,z}^* + a_{s,z}b_{s,x}^*]. \tag{C24}
\end{aligned}$$

3. Spine cross-tie interactions

Here we analyze the spin-cross tie interactions.

We consider the terms proportional to L_{xx}^y :

$$\begin{aligned}
V_y(L_{xx}^y) &= Q_y L_{xx}^y [S_x(5) + S_x(6)] \\
&\quad \times [S_x(1) - S_x(2) - S_x(3) + S_x(4)] \\
&\equiv N_{uc} Q_y L_{xx}^y [u_{xx} + u_{xx}^*], \tag{C25}
\end{aligned}$$

where

$$\begin{aligned}
u_{xx} &= b_{cx} [(a_{s,x}^* - ib_{s,x}^*)e^{-iqa/4} \\
&\quad - (-a_{s,x}^* - ib_{s,x}^*)e^{-iqa/4} - (a_{s,x}^* + ib_{s,x}^*)e^{iqa/4} \\
&\quad + (-a_{s,x}^* + ib_{s,x}^*)e^{iqa/4} \\
&\quad - (a_{s,x}^* - ib_{s,x}^*)e^{iqa/4} + (-a_{s,x}^* - ib_{s,x}^*)e^{iqa/4} \\
&\quad + (a_{s,x}^* + ib_{s,x}^*)e^{-iqa/4} - (-a_{s,x}^* + ib_{s,x}^*)e^{-iqa/4}] \\
&= 4b_{cx}a_{s,x}^* [e^{-iqa/4} - e^{iqa/4}] \\
&= -8i \sin(qa/4) b_{cx} a_{s,x}^* \tag{C26}
\end{aligned}$$

so that

$$V_y(L_{xx}^y) = 16N_{uc}Q_y L_{xx}^y \sin(qa/4) \Im[b_{cx}a_{s,x}^*] \tag{C27}$$

We consider the terms proportional to L_{yy}^y :

$$\begin{aligned}
V_y(L_{yy}^y) &= Q_y L_{yy}^y [S_y(5) + S_y(6)] \\
&\quad [S_y(1) - S_y(2) - S_y(3) + S_y(4)] \\
&\equiv N_{uc} Q_y L_{yy}^y [u_{yy} + u_{yy}^*], \tag{C28}
\end{aligned}$$

where

$$\begin{aligned}
u_{yy} &= a_{cy} [(-ia_{s,y}^* + b_{s,y}^*)e^{-iqa/4} - (-ia_{s,y}^* - b_{s,y}^*)e^{-iqa/4} \\
&\quad - (ia_{s,y}^* + b_{s,y}^*)e^{iqa/4} + (ia_{s,y}^* - b_{s,y}^*)e^{iqa/4} \\
&\quad - (-ia_{s,y}^* + b_{s,y}^*)e^{iqa/4} + (-ia_{s,y}^* - b_{s,y}^*)e^{iqa/4} \\
&\quad + (ia_{s,y}^* + b_{s,y}^*)e^{-iqa/4} - (ia_{s,y}^* - b_{s,y}^*)e^{-iqa/4}] \\
&= 4a_{cy}b_{s,y}^* [e^{-iqa/4} - e^{iqa/4}] \\
&= -8i \sin(qa/4) a_{cy} b_{s,y}^* \tag{C29}
\end{aligned}$$

so that

$$V_y(L_{yy}^y) = 16N_{uc}Q_y L_{yy}^y \sin(qa/4) \Im[a_{cy}b_{s,y}^*] \tag{C30}$$

We consider the terms proportional to L_{zz}^y :

$$\begin{aligned}
V_y(L_{zz}^y) &= Q_y L_{zz}^y [S_z(5) + S_z(6)] \\
&\quad \times [S_z(1) - S_z(2) - S_z(3) + S_z(4)] \\
&\equiv N_{uc} Q_y L_{zz}^y [u_{zz} + u_{zz}^*], \tag{C31}
\end{aligned}$$

where

$$\begin{aligned}
u_{zz} &= a_{cz} [(a_{s,z}^* - ib_{s,z}^*)e^{-iqa/4} - (a_{s,z}^* + ib_{s,z}^*)e^{-iqa/4} \\
&\quad - (a_{s,z}^* + ib_{s,z}^*)e^{iqa/4} + (a_{s,z}^* - ib_{s,z}^*)e^{iqa/4} \\
&\quad + (a_{s,z}^* - ib_{s,z}^*)e^{iqa/4} - (a_{s,z}^* + ib_{s,z}^*)e^{iqa/4} \\
&\quad - (a_{s,z}^* + ib_{s,z}^*)e^{-iqa/4} + (a_{s,z}^* - ib_{s,z}^*)e^{-iqa/4}] \\
&= 4a_{cz}b_{s,z}^* i [-e^{-iqa/4} - e^{iqa/4}] \\
&= -8ia_{cz}b_{s,z}^* \cos(aq/4), \tag{C32}
\end{aligned}$$

so that

$$V_y(L_{zz}^y) = 16N_{uc}Q_yL_{zz}^y \cos(qa/4)\Im[a_{cz}b_{s,z}^*]. \quad (C33)$$

We consider the terms proportional to L_{xy}^y :

$$\begin{aligned} V_y(L_{xy}^y) &= Q_yL_{xy}^y \left([S_x(5) - S_x(6)] \right. \\ &\quad \times [S_y(1) + S_y(2) - S_y(3) - S_y(4)] \\ &\quad + [S_y(5) - S_y(6)] \\ &\quad \left. \times [S_x(1) + S_x(2) - S_x(3) - S_x(4)] \right) \\ &\equiv N_{uc}Q_yL_{xy}^y[u_{xy} + u_{xy}^*], \quad (C34) \end{aligned}$$

where

$$\begin{aligned} u_{xy} &= b_{cx} \left[(-ia_{s,y}^* + b_{s,y}^*)e^{-iqa/4} + (-ia_{s,y}^* - b_{s,y}^*)e^{-iqa/4} \right. \\ &\quad - (ia_{s,y}^* + b_{s,y}^*)e^{iqa/4} - (ia_{s,y}^* - b_{s,y}^*)e^{iqa/4} \\ &\quad + (-ia_{s,y}^* + b_{s,y}^*)e^{iqa/4} + (-ia_{s,y}^* - b_{s,y}^*)e^{iqa/4} \\ &\quad \left. - (ia_{s,y}^* + b_{s,y}^*)e^{-iqa/4} - (ia_{s,y}^* - b_{s,y}^*)e^{-iqa/4} \right] \\ &\quad + a_{cy} \left[(a_{s,x}^* - ib_{s,x}^*)e^{-iqa/4} \right. \\ &\quad + (-a_{s,x}^* - ib_{s,x}^*)e^{-iqa/4} - (a_{s,x}^* + ib_{s,x}^*)e^{iqa/4} \\ &\quad - (-a_{s,x}^* + ib_{s,x}^*)e^{iqa/4} \\ &\quad + (a_{s,x}^* - ib_{s,x}^*)e^{iqa/4} + (-a_{s,x}^* - ib_{s,x}^*)e^{iqa/4} \\ &\quad \left. - (a_{s,x}^* + ib_{s,x}^*)e^{-iqa/4} - (-a_{s,x}^* + ib_{s,x}^*)e^{-iqa/4} \right] \\ &= 4ib_{cx} \left[-a_{s,y}^*e^{-iqa/4} - a_{s,y}^*e^{iqa/4} \right] \\ &\quad + 4ia_{cy} \left[-b_{s,x}^*e^{-iqa/4} - b_{s,x}^*e^{iqa/4} \right] \\ &= -8i[b_{cx}a_{s,y}^* + a_{cy}b_{s,x}^*] \cos(qa/4), \quad (C35) \end{aligned}$$

so that

$$\begin{aligned} V_y(L_{xy}^y) &= 16N_{uc}Q_yL_{xy}^y \cos(qa/4) \\ &\quad \times \Im[b_{cx}a_{s,y}^* + a_{cy}b_{s,x}^*]. \quad (C36) \end{aligned}$$

We consider the terms proportional to L_{xz}^y :

$$\begin{aligned} V_y(L_{xz}^y) &= Q_yL_{xz}^y \left([S_x(5) + S_x(6)] \right. \\ &\quad \times [S_z(1) + S_z(2) - S_z(3) - S_z(4)] \\ &\quad + [S_z(5) + S_z(6)] \\ &\quad \left. \times [S_x(1) + S_x(2) - S_x(3) - S_x(4)] \right) \\ &\equiv N_{uc}Q_yL_{xz}^y[u_{xz} + u_{xz}^*], \quad (C37) \end{aligned}$$

where

$$\begin{aligned} u_{xz} &= b_{cx} \left[(a_{s,z}^* - ib_{s,z}^*)e^{-iqa/4} + (a_{s,z}^* + ib_{s,z}^*)e^{-iqa/4} \right. \\ &\quad \left. - (a_{s,z}^* + ib_{s,z}^*)e^{iqa/4} - (a_{s,z}^* - ib_{s,z}^*)e^{iqa/4} \right] \end{aligned}$$

$$\begin{aligned} &- (a_{s,z}^* - ib_{s,z}^*)e^{iqa/4} - (a_{s,z}^* + ib_{s,z}^*)e^{iqa/4} \\ &+ (a_{s,z}^* + ib_{s,z}^*)e^{-iqa/4} + (a_{s,z}^* - ib_{s,z}^*)e^{-iqa/4} \\ &+ a_{cz} \left[(a_{s,x}^* - ib_{s,x}^*)e^{-iqa/4} \right. \\ &\quad + (-a_{s,x}^* - ib_{s,x}^*)e^{-iqa/4} \\ &\quad - (a_{s,x}^* + ib_{s,x}^*)e^{iqa/4} - (-a_{s,x}^* + ib_{s,x}^*)e^{iqa/4} \\ &\quad + (a_{s,x}^* - ib_{s,x}^*)e^{iqa/4} + (-a_{s,x}^* - ib_{s,x}^*)e^{iqa/4} \\ &\quad \left. - (a_{s,x}^* + ib_{s,x}^*)e^{-iqa/4} - (-a_{s,x}^* + ib_{s,x}^*)e^{-iqa/4} \right] \\ &= 4b_{cx}a_{s,z}^* [e^{-iqa/4} - e^{-iqa/4}] \\ &\quad + 4a_{cz}b_{s,x}^* [-ie^{-iqa/4} - ie^{iqa/4}] \\ &= -8ib_{cx}a_{s,z}^* \sin(qa/4) - 8ia_{cz}b_{s,x}^* \cos(qa/4), \quad (C38) \end{aligned}$$

so that

$$\begin{aligned} V_y(L_{xz}^y) &= 16N_{uc}Q_yL_{xz}^y \left(\sin(qa/4)\Im[b_{cx}a_{s,z}^*] \right. \\ &\quad \left. + \cos(qa/4)\Im[a_{cz}b_{s,x}^*] \right). \quad (C39) \end{aligned}$$

We consider the terms proportional to L_{yz}^y :

$$\begin{aligned} V_y(L_{yz}^y) &= Q_yL_{yz}^y \left([S_y(5) - S_y(6)] \right. \\ &\quad \times [S_z(1) - S_z(2) - S_z(3) + S_z(4)] \\ &\quad + [S_z(5) - S_z(6)] \\ &\quad \left. \times [S_y(1) - S_y(2) - S_y(3) + S_y(4)] \right) \\ &\equiv N_{uc}Q_yL_{yz}^y[u_{yz} + u_{yz}^*], \quad (C40) \end{aligned}$$

where

$$\begin{aligned} u_{yz} &= a_{cy} \left[(a_{s,z}^* - ib_{s,z}^*)e^{-iqa/4} - (a_{s,z}^* + ib_{s,z}^*)e^{-iqa/4} \right. \\ &\quad - (a_{s,z}^* + ib_{s,z}^*)e^{iqa/4} + (a_{s,z}^* - ib_{s,z}^*)e^{iqa/4} \\ &\quad + (a_{s,z}^* - ib_{s,z}^*)e^{iqa/4} - (a_{s,z}^* + ib_{s,z}^*)e^{iqa/4} \\ &\quad \left. - (a_{s,z}^* + ib_{s,z}^*)e^{-iqa/4} + (a_{s,z}^* - ib_{s,z}^*)e^{-iqa/4} \right] \\ &\quad + a_{c,z} \left[(-ia_{s,y}^* + b_{s,y}^*)e^{-iqa/4} \right. \\ &\quad - (-ia_{s,y}^* - b_{s,y}^*)e^{-iqa/4} \\ &\quad - (ia_{s,y}^* + b_{s,y}^*)e^{iqa/4} + (ia_{s,y}^* - b_{s,y}^*)e^{iqa/4} \\ &\quad - (-ia_{s,y}^* + b_{s,z}^*)e^{iqa/4} + (-ia_{s,y}^* - b_{s,y}^*)e^{iqa/4} \\ &\quad \left. + (ia_{s,y}^* + b_{s,y}^*)e^{-iqa/4} - (ia_{s,y}^* - b_{s,y}^*)e^{-iqa/4} \right] \\ &= -4ia_{cy}b_{s,z}^* [e^{-iqa/4} + e^{iqa/4}] \\ &\quad + 4a_{c,z}b_{s,y}^* [e^{-iqa/4} - e^{iqa/4}] \\ &= -8ia_{cy}b_{s,z}^* \cos(aq/4) - 8ia_{c,z}b_{s,y}^* \sin(qa/4), \quad (C41) \end{aligned}$$

so that

$$V_y(L_{yz}^y) = 16N_{uc}Q_yL_{yz}^y \left(\cos(qa/4)\Im[a_{cy}b_{s,z}^*] + \sin(qa/4)\Im[a_{cz}b_{s,y}^*] \right). \quad (C42)$$

We consider the terms proportional to F_x^y :

$$\begin{aligned} V_y(F_x^y) &= Q_yF_x^y \left([S_y(5) - S_y(6)] \right. \\ &\quad \times [S_z(1) - S_z(2) - S_z(3) + S_z(4)] \\ &\quad \left. - [S_z(5) - S_z(6)] \right. \\ &\quad \left. \times [S_y(1) - S_y(2) - S_y(3) + S_y(4)] \right) \\ &\equiv N_{uc}Q_yF_x^y[u_x + u_x^*], \end{aligned} \quad (C43)$$

where

$$\begin{aligned} u_x &= a_{cy} \left[(a_{s,z}^* - ib_{s,z}^*)e^{-iqa/4} - (a_{s,z}^* + ib_{s,z}^*)e^{-iqa/4} \right. \\ &\quad \left. - (a_{s,z}^* + ib_{s,z}^*)e^{iqa/4} + (a_{s,z}^* - ib_{s,z}^*)e^{iqa/4} \right. \\ &\quad \left. + (a_{s,z}^* - ib_{s,z}^*)e^{iqa/4} - (a_{s,z}^* + ib_{s,z}^*)e^{iqa/4} \right. \\ &\quad \left. - (a_{s,z}^* + ib_{s,z}^*)e^{-iqa/4} + (a_{s,z}^* - ib_{s,z}^*)e^{-iqa/4} \right] \\ &\quad + a_{cz} \left[-(-ia_{s,y}^* + b_{s,y}^*)e^{-iqa/4} \right. \\ &\quad \left. + (-ia_{s,y}^* - b_{s,y}^*)e^{-iqa/4} \right. \\ &\quad \left. + (ia_{s,y}^* + b_{s,y}^*)e^{iqa/4} - (ia_{s,y}^* - b_{s,y}^*)e^{iqa/4} \right. \\ &\quad \left. + (-ia_{s,y}^* + b_{s,y}^*)e^{iqa/4} - (-ia_{s,y}^* - b_{s,y}^*)e^{iqa/4} \right. \\ &\quad \left. - (ia_{s,y}^* + b_{s,y}^*)e^{-iqa/4} + (ia_{s,y}^* - b_{s,y}^*)e^{-iqa/4} \right] \\ &= -4ia_{cy}b_{s,z}^* \left[e^{-iqa/4} + e^{iqa/4} \right] \\ &\quad + 4a_{cz}b_{s,y}^* \left[e^{iqa/4} - e^{-iqa/4} \right] \\ &= -8ia_{cy}b_{s,z}^* \cos(qa/4) + 8ia_{cz}b_{s,y}^* \sin(qa/4), \end{aligned} \quad (C44)$$

so that

$$\begin{aligned} V_y(F_x^y) &= 16N_{uc}Q_yF_x^y \left(\cos(qa/4)\Im[a_{cy}b_{s,z}^*] \right. \\ &\quad \left. + \sin(qa/4)\Im[a_{cz}b_{s,y}^*] \right). \end{aligned} \quad (C45)$$

We consider the terms proportional to F_y^y :

$$\begin{aligned} V_y(F_y^y) &= Q_yF_y^y \left(-[S_x(5) + S_x(6)] \right. \\ &\quad \times [S_z(1) + S_z(2) - S_z(3) - S_z(4)] \\ &\quad \left. + [S_z(5) + S_z(6)] \right. \\ &\quad \left. \times [S_x(1) + S_x(2) - S_x(3) - S_x(4)] \right) \\ &\equiv N_{uc}Q_yL_{yz}^y[u_y + u_y^*], \end{aligned} \quad (C46)$$

where

$$\begin{aligned} u_y &= b_{cx} \left[-(a_{s,z}^* - ib_{s,z}^*)e^{-iqa/4} - (a_{s,z}^* + ib_{s,z}^*)e^{-iqa/4} \right. \\ &\quad \left. + (a_{s,z}^* + ib_{s,z}^*)e^{iqa/4} + (a_{s,z}^* - ib_{s,z}^*)e^{iqa/4} \right. \\ &\quad \left. + (a_{s,z}^* - ib_{s,z}^*)e^{iqa/4} + (a_{s,z}^* + ib_{s,z}^*)e^{iqa/4} \right. \\ &\quad \left. - (a_{s,z}^* + ib_{s,z}^*)e^{-iqa/4} - (a_{s,z}^* - ib_{s,z}^*)e^{-iqa/4} \right] \\ &\quad + a_{c,z} \left[(a_{s,x}^* - ib_{s,x}^*)e^{-iqa/4} \right. \\ &\quad \left. + (-a_{s,x}^* - ib_{s,x}^*)e^{-iqa/4} \right. \\ &\quad \left. - (a_{s,x}^* + ib_{s,x}^*)e^{iqa/4} - (-a_{s,x}^* + ib_{s,x}^*)e^{iqa/4} \right. \\ &\quad \left. (a_{s,x}^* - ib_{s,x}^*)e^{iqa/4} + (-a_{s,x}^* - ib_{s,x}^*)e^{iqa/4} \right. \\ &\quad \left. - (a_{s,x}^* + ib_{s,x}^*)e^{-iqa/4} - (-a_{s,x}^* + ib_{s,x}^*)e^{-iqa/4} \right] \\ &= 4b_{cx}a_{s,z}^* \left[-e^{-iqa/4} + e^{iqa/4} \right] \\ &\quad + 4a_{c,z}b_{s,x}^* \left[-ie^{-iqa/4} - ie^{iqa/4} \right] \\ &= 8ib_{cx}a_{s,z}^* \sin(qa/4) - 8ia_{c,z}b_{s,x}^* \cos(aq/4), \end{aligned} \quad (C47)$$

so that

$$\begin{aligned} V_y(F_y^y) &= 16N_{uc}Q_yF_y^y \left(\sin(qa/4)\Im[b_{cx}a_{s,z}^*] \right. \\ &\quad \left. + \cos(aq/4)\Im[a_{c,z}b_{s,x}^*] \right). \end{aligned} \quad (C48)$$

Finally, we consider the terms proportional to F_z^y :

$$\begin{aligned} V_y(F_z^y) &= Q_yF_z^y \left([S_x(5) - S_x(6)] \right. \\ &\quad \times [S_y(1) + S_y(2) - S_y(3) - S_y(4)] \\ &\quad \left. - [S_y(5) - S_y(6)] \right. \\ &\quad \left. \times [S_x(1) + S_x(2) - S_x(3) - S_x(4)] \right) \\ &\equiv N_{uc}Q_yF_z^y[u_z + u_z^*], \end{aligned} \quad (C49)$$

where

$$\begin{aligned} u_z &= b_{cx} \left[(-ia_{s,y}^* + b_{s,y}^*)e^{-iqa/4} \right. \\ &\quad \left. + (-ia_{s,y}^* - b_{s,y}^*)e^{-iqa/4} \right. \\ &\quad \left. - (ia_{s,y}^* + b_{s,y}^*)e^{iqa/4} - (ia_{s,y}^* - b_{s,y}^*)e^{iqa/4} \right. \\ &\quad \left. + (-ia_{s,y}^* + b_{s,y}^*)e^{iqa/4} + (-ia_{s,y}^* - b_{s,y}^*)e^{iqa/4} \right. \\ &\quad \left. - (ia_{s,y}^* + b_{s,y}^*)e^{-iqa/4} - (ia_{s,y}^* - b_{s,y}^*)e^{-iqa/4} \right] \\ &\quad + a_{c,y} \left[-(a_{s,x}^* - ib_{s,x}^*)e^{-iqa/4} \right. \\ &\quad \left. - (-a_{s,x}^* - ib_{s,x}^*)e^{-iqa/4} \right. \\ &\quad \left. + (a_{s,x}^* + ib_{s,x}^*)e^{iqa/4} + (-a_{s,x}^* + ib_{s,x}^*)e^{iqa/4} \right. \\ &\quad \left. - (a_{s,x}^* - ib_{s,x}^*)e^{iqa/4} - (-a_{s,x}^* - ib_{s,x}^*)e^{iqa/4} \right] \end{aligned}$$

$$\begin{aligned}
& +(a_{s,x}^* + ib_{s,x}^*)e^{-iq/4} + (-a_{s,x}^* + ib_{s,x}^*)e^{-iq/4} \\
= & 4ib_{cx}a_{s,y}^* \left[-e^{-iq/4} - e^{iq/4} \right] \\
& + 4ia_{cy}b_{s,x}^* \left[e^{-iq/4} + e^{iq/4} \right] \\
= & -8ib_{cx}a_{s,y}^* \cos(q/4) + 8ia_{cy}b_{s,x}^* \cos(q/4), \quad (\text{C50})
\end{aligned}$$

so that

$$\begin{aligned}
V_y(F_z^y) = & 16N_{uc}Q_yF_z^y \cos(q/4) \\
& \times \Im[b_{cx}a_{s,y}^* + a_{cy}^*b_{s,x}]. \quad (\text{C51})
\end{aligned}$$

-
- ¹ N. Rogado, G. Lawes, D. A. Huse, A. P. Ramirez, and R. J. Cava, *Solid State Comm.* **124**, 229 (2002).
- ² G. Lawes, M. Kenzelmann, N. Rogado, K. H. Kim, G. A. Jorge, R. J. Cava, A. Aharony, O. Entin-Wohlman, A. B. Harris, T. Yildirim, Q. A. Huang, S. Park, C. Broholm, and A. P. Ramirez, *Phys. Rev. Lett.* **93**, 247201 (2004).
- ³ G. Lawes, A. B. Harris, T. Kimura, N. Rogado, R. J. Cava, A. Aharony, O. Entin-Wohlman, T. Yildirim, M. Kenzelmann, C. Broholm, and A. P. Ramirez, *Phys. Rev. Lett.* **95**, 087205 (2005).
- ⁴ M. Kenzelmann, A. B. Harris, A. Aharony, O. Entin-Wohlman, T. Yildirim, Q. Huang, S. Park, G. Lawes, C. Broholm, N. Rogado, R. J. Cava, K. H. Kim, G. Jorge, and A. P. Ramirez, *cond-mat/0509xxx*.
- ⁵ N. Hur, S. Park, P. A. Sharma, J. S. Ahn, S. Guha, and S.-W. Cheong, *Nature* **429**, 392 (2004).
- ⁶ M. Kenzelmann, A. B. Harris, S. Jonas, C. Broholm, J. Schefer, S. B. Kim, C. L. Zhang, S.-W. Cheong, O. P. Vajk, and J. W. Lynn, *Phys. Rev. Lett.* **95**, 087206 (2005).
- ⁷ A. B. Harris and G. Lawes, *Ferroelectricity in Incommensurate Magnets*, in *The Handbook of Magnetism and Advanced Magnetic Materials*, (J. Wiley, London, 2006); *cond-mat/0508617*; A. B. Harris, *cond-mat/0508730*.
- ⁸ I. Dzyaloshinskii, *J. Phys. Chem. Solids* **4**, 241 (1958).
- ⁹ T. Moriya, *Phys. Rev.* **120**, 91 (1960).
- ¹⁰ I. A. Sergienko and E. Dagotto, *cond-mat/0508075*.
- ¹¹ P. C. Hohenberg and W. Kohn, *Phys. Rev.* **136**, B864 (1964); W. Kohn and L. J. Sham, *Phys. Rev.* **140**, A1133 (1965).
- ¹² V. I. Anisimov, F. Aryasetiawan, and A. I. Lichtenstein, *J. Phys. Cond. Matter* **9**, 767 (1997).
- ¹³ A. J. C. Wilson, *International Tables For Crystallography* (Kluwer Academic Publishers, Dordrecht, 1995), Vol. A.
- ¹⁴ E. E. Sauerbrei, F. Faggiani, and C. Calvo, *Acta Crystallogr. B* **29**, 2304 (1973).
- ¹⁵ P. W. Anderson, *Phys. Rev.* **115**, 2 (1959).
- ¹⁶ T. Yildirim, A. B. Harris, A. Aharony, and O. Entin-Wohlman, *Phys. Rev. B* **52**, 10239 (1996).
- ¹⁷ O. Entin-Wohlman, A. B. Harris, and A. Aharony, *Phys. Rev. B* **53**, 11661 (1996).
- ¹⁸ R. Schmitz, O. Entin-Wohlman, A. Aharony, A. B. Harris, and E. Müller-Hartmann, *Phys. Rev. B* **71**, 144412 (2005).
- ¹⁹ R. Schmitz, O. Entin-Wohlman, A. Aharony, A. B. Harris, and E. Müller-Hartmann, *Phys. Rev. B* **71**, 214438 (2005).
- ²⁰ J. R. D. Copley, D. A. Neumann, W. A. Kamitakahara, *Can. J. Phys.* **73**, 763 (1995).
- ²¹ S. Baroni, A. Dal Corso, S. de Gironcoli, and P. Giannozzi, <http://www.pwscf.org>
- ²² T. Yildirim, *Chem. Phys.* **261**, 205 (2000).
- ²³ Animations of the B_{2u} phonons can be found at <http://www.ncnr.nist.gov/staff/taner/nvo>
- ²⁴ E. P. Wigner, *Group Theory*. (Academic Press, New York, 1959). M. Tinkham, *Group Theory and Quantum Mechanics*, (McGraw-Hill, New York, 1964).
- ²⁵ A. B. Harris *et al.*, unpublished.